Breaking Orthogonality in Uplink With Randomly Deployed Sources

APOSTOLOS A. TEGOS[1], SOTIRIS A. TEGOS [ID] (Member, IEEE),
DIMITRIOS TYROVOLAS [ID][1,2] (Graduate Student Member, IEEE),
PANAGIOTIS D. DIAMANTOULAKIS [ID][1] (Senior Member, IEEE),
PANAGIOTIS SARIGIANNIDIS [ID][1] (Member, IEEE),
AND GEORGE K. KARAGIANNIDIS [ID][1,3] (Fellow, IEEE)

[1]Department of Electrical and Computer Engineering, Aristotle University of Thessaloniki, 54124 Thessaloniki, Greece

[2]Department of Informatics and Telecommunication Engineering, University of Western Macedonia, 50100 Kozani, Greece

[3]Artificial Intelligence and Cyber Systems Research Center, Lebanese American University, Beirut, Lebanon

CORRESPONDING AUTHOR: S. A. TEGOS (e-mail: sotiristegos@ieee.org)

ABSTRACT The requirement of the upcoming sixth-generation (6G) wireless communication systems to significantly elevate the services of enhanced mobile broadband (eMBB) and massive machine-type communications (mMTC) necessitates the design and investigation of appropriate multiple access schemes. This paper investigates the impact of random source deployment on the performance of uplink systems, emphasizing the implications of non-orthogonality in contention-free and contention-based access schemes. For the latter scheme, we combine the strengths of slotted ALOHA and successive interference cancellation. Considering the advantages of breaking orthogonality in scenarios with random source deployment, we propose distinct policies tailored for mMTC, eMBB, and hybrid mMTC-eMBB scenarios by splitting the cell into rings. Furthermore, we derive closed-form expressions for the outage probability, which play a pivotal role in extracting the throughput of the sources in the considered scenarios. The paper offers a comprehensive analysis of the proposed approach, corroborated through simulations, shedding light on the potential of such protocols in future 6G wireless communication systems.

INDEX TERMS Random access, slotted ALOHA, NOMA, SIC, randomly distributed sources, outage probability, throughput, mMTC, eMBB, user pairing.

I. INTRODUCTION

A KEY objective of the sixth-generation (6G) of wireless networks is to substantially improve the classes of services offered by the 5G, including enhanced mobile broadband (eMBB) and massive machine-type communications (mMTC). As the wireless landscape evolves, the emergence of technologies like network slicing and open radio access network (Open RAN) underscores the importance of design and investigation of advanced multiple access schemes, emphasizing flexibility and interoperability in network deployments [1], [2], [3]. Multiple access can be classified into two main categories, namely contention-free (CF) and contention-based (CB) ones, in which the resources are allocated in a coordinated or in an opportunistic way, respectively. In eMBB, CF schemes are preferred, since the target objective is spectral efficiency, while CB offers advantages in mMTC, where scalability is the main challenge. This is because in mMTC applications, e.g., Internet of Things (IoT), the activity of the sources is usually sparse, rendering centralized coordination inefficient due to under-utilization of the available resources and extremely high overhead requirements [4], [5], [6], [7]. Taking the aforementioned into account, in existing eMBB applications orthogonal multiple access is the dominant technology, while in mMTC

applications, random access (RA) is considered as the most promising approach. This is because RA also offers low latency for small payload transmissions, without requiring initial connection setup or dedicated resource allocation for connection maintenance.

Compared to other RA protocols, slotted ALOHA (SA) [8] performs more efficiently by avoiding collisions due to partially overlapping transmissions while maintaining low complexity. Specifically, an SA network is assumed to comprise identical and independently operating sources. The behavior of each terminal is described by the origination and transmission state. A source, in the origination state, transmits a packet in the next time slot with a certain access probability. If successful, it receives a positive acknowledgment and returns to the origination state, otherwise, a collision occurs. Consequently, SA is implemented in a variety of applications in different wireless setups [9], [10]. However, SA may suffer from congestion as the traffic load and the number of sources increase.

A. MOTIVATION

To increase spectral efficiency and massive connectivity in future generations of wireless networks, breaking the requirement of orthogonality is a promising approach [11]. To break orthogonality, multi-user detection techniques such as successive interference cancellation (SIC) which is the basis of power domain non-orthogonal multiple access (NOMA), are required to retrieve the sources' signals at the receiver [12]. In SIC, the signal of one source is decoded by treating the signals of other sources as interference and, if successfully decoded, subtracted from the superimposed received signal. Uplink NOMA extends the capacity region compared to orthogonal multiple access (OMA), which can lead to increased spectral efficiency. In this context, the use of SIC is critical in RA, since it can be used to reduce the number of collisions as collided messages can still be decoded. Thus, leveraging the capabilities of SA and SIC offers a promising way to address congestion challenges.

However, to understand the benefit of breaking orthogonality, practical aspects should be considered, including random source deployment, which has been overlooked in the existing literature. Specifically, random source deployment captures the variability and unpredictability inherent in real-world deployments, where sources are randomly deployed, providing a more accurate basis for scenarios involving sources with both homogeneous, e.g., eMBB-emBB, mMTC-mMTC, and heterogeneous, e.g., mMTC-eMBB, requirements. To this end, appropriate policies for geometry-aware resource management should also be proposed to design appropriate centralized, opportunistic, or hybrid medium access control schemes, including both CF and CB access.

B. CONTRIBUTION

Motivated by the above, we investigate the impact of random source deployment on the performance of uplink

systems, particularly focusing on the implications of non-orthogonality in CF and CB access schemes. Specifically, we examine a network with sources randomly and uniformly distributed in ring configurations, addressing a critical gap in the existing literature that often overlooks practical deployment scenarios. Furthermore, our work highlights unique challenges differing from fixed user location scenarios and ensures an unbiased analysis, which is essential to meet the diverse user requirements in various deployment contexts. Specifically, the contributions of this work are as follows:

- Considering the advantages of breaking orthogonality in scenarios with random source deployment, we propose different policies for mMTC, eMBB, and hybrid mMTC-eMBB scenarios, focusing on both homogeneous and heterogeneous requirements and enabling geometry-aware resource management. To investigate the performance of the proposed policies, three different cases are identified by splitting the cell into different rings. For each scenario, we employ either a CF or a CB access scheme. Specifically, we utilize as a CB access scheme a protocol based on the combination of SA with SIC, termed as SA-SIC, which efficiently reduces the number of collisions.

- Closed-form expressions for the outage probability of the system are derived for the three source deployment cases. Using these expressions, the throughput of the sources for the proposed policies is presented.

- The theoretical analysis is validated by simulation results, which also illustrate the superiority of the considered CB access scheme over conventional SA and highlight the impact of random source deployment in CF and CB schemes. The numerical results provide useful design insights into the considered policies, e.g., that different access probabilities for sources distributed in different rings can lead to improved performance both in terms of overall performance and fairness. To this end, practical user-pairing schemes are extracted for the investigated scenarios.

C. STRUCTURE

The remainder of the paper is organized as follows: Section II provides the related works, while Section III describes the system model. In Section IV, the performance analysis of the considered system in terms of outage probability and throughput is provided. In Section V, simulation results are provided to verify the derived analytical results and to illustrate the system performance, while Section VI concludes the paper.

II. RELATED WORKS

Several studies have explored the advantages of power domain NOMA over orthogonal multiple access [13], [14], [15], [16]. Given the escalating decoding complexity of NOMA as the number of multiplexed messages grows, a practical approach to NOMA involves hybrid user pairing. In this approach, a maximum of two

users can share the same resource block, while different user pairs utilize orthogonal resources [17]. This NOMA variant is consistent with its application in the 3rd Generation Partnership Project (3GPP) standards [18]. While there is extensive research on downlink NOMA, uplink NOMA remains relatively underexplored. It is worth noting that uplink NOMA differs significantly from its downlink counterpart, primarily because interfering messages in uplink come from different sources. Implementing NOMA in the uplink does not add extra complexity for users, since joint processing is performed exclusively at the base station (BS). For instance, [19] examined the ergodic sum-rate advantage of NOMA over OMA, shedding light on the scalability of the gain with increasing number of antennas. Furthermore, determining the outage probability for uplink NOMA is crucial as it lays the foundation for the design and optimization of practical medium access control (MAC) schemes. In this context, the outage probability for uplink NOMA with both single-antenna and multi-antenna BSs was established in [20] and [21], respectively, assuming stationary user positions.

Considering their advantages, i.e., the simplicity of ALOHA as well as the improved throughput of NOMA and its ability to avoid collisions utilizing multi-user detection techniques, a hybrid ALOHA-NOMA scheme can be considered as an efficient alternative MAC protocol for low-complexity IoT devices. Specifically, in [22] and [23], it was proven that the main drawbacks of ALOHA, i.e., low throughput and high collision rate, can be mitigated by NOMA. In [22], a NOMA-based RA scheme with multichannel ALOHA was examined, where users can choose predetermined power levels to transmit their information. By using SIC with perfect channel state information (CSI), the co-channel interference is mitigated. It was also shown that NOMA can be employed for uncoordinated transmissions such as RA in IoT networks. In [24] and [25], the performance of a similar protocol was evaluated. Specifically, in [24], it was shown that this protocol outperforms the carrier sensing multiple access with collision avoidance (CSMA/CA) in terms of throughput at low transmission probability at the cost of increased average delay, while in [25] its superiority over SA was demonstrated. Moreover, the authors of [26] investigated the performance of SA-NOMA using SIC in IoT networks. To improve the performance, an enhanced SA-NOMA receiver was proposed, which calculates the number of active devices using a form of multi-hypothesis testing. Finally, in [20], two RA protocols based on SA and uplink NOMA were proposed utilizing both SIC with optimal decoding order and joint decoding (JD). The average throughput and the corresponding outage probability of the proposed protocols were derived and the improvement over was proven.

Despite the aforementioned advances, none of these works explores the practical case in the context of IoT mMTC applications where sources are randomly deployed [27].

For instance, [28] aimed to balance spatial reuse and per-transmitter throughput in networks with randomly deployed stations, deriving closed-form expressions for various spatial averages. In addition, [29] focused on an RA network with spatial reuse, aiming for optimal signal-to-interference-plus-noise ratio (SINR) in an SA system with node locations determined by a two-dimensional Poisson point process. Furthermore, [30] and [31] explored NOMA networks with random user deployment, with the former proposing an efficient cooperative relay sharing strategy, while [14] assessed the performance of NOMA in a cellular downlink scenario with random users, noting its superior ergodic sum rates. This was later extended in [32], which generalized the findings for various fading distributions and presented a closed-form analysis for the case of Nakagami-m fading. However, to the best of the authors' knowledge, the existing literature does not include closed-form expressions for the outage probability and the throughput of SA-NOMA schemes utilizing SIC with randomly deployed users. In this direction, given the inherent variability of IoT sensor deployments, it becomes crucial to employ random user distribution to understand system performance in all conceivable deployment scenarios. This comprehensive analysis not only characterizes the potential and versatility of SA-NOMA in diverse real-world IoT environments, but also paves the way to derive the optimal design parameters of the protocol, ultimately leading to improved network performance.

III. SYSTEM MODEL AND PROPOSED SCHEMES

In this work, we examine the performance of a network with randomly deployed sources to cover the inherent unpredictability of device placements in real-world applications. To this end, we consider a network comprising a single-antenna BS that possesses perfect CSI and N single-antenna sources experiencing Rayleigh fading. The purposeful adoption of single-antenna nodes, perfect CSI, and Rayleigh fading facilitates clear and precise derivation of outage probabilities, directly addressing the essential aspects of the scenarios under investigation. Furthermore, the selection of these assumptions not only ensures a robust analysis but also suggests that the relative performance trends among the examined scenarios would consistently hold, even with multiple antennas, the integration of CSI imperfections, and different fading conditions.

Delving deeper, the sources in the examined model transmit signals within structured time intervals, with time systematically divided into frames. Consequently, the received signal-to-noise ratio (SNR) of the i-th source is described by

$$\gamma_i = \frac{l_i |h_i|^2 p_i}{\sigma^2}, \tag{1}$$

where σ^2, h_i and p_i denote the variance of the additive white Gaussian noise (AWGN), the small scale fading coefficient

between the i-th source and the BS, and the transmitted power of the i-th source, respectively, while

$$l_i = cd_i^{-n} \qquad (2)$$

expresses the path loss factor with c, d_i, and n denote the path loss at reference distance d_0, the distance between the i-th source and the BS, and the path loss exponent, respectively. We assume Rayleigh fading, thus $|h_i|^2$ follows the exponential distribution with rate parameter 1 and γ_i follows the exponential distribution with rate parameter $b_i = \frac{\sigma^2}{l_i p_i}$.

To examine the performance of a network with randomly deployed sources, an appropriate model for the sources' locations is essential. Therefore, considering that the sources are uniformly distributed in a circular ring, whose center coincides with the BS, the distance between the i-th source and the BS is a random variable with cumulative distribution function (CDF) given as

$$F_{d_i}(x) = \frac{x^2 - r^2}{R^2 - r^2}, \quad x \in [r, R], \qquad (3)$$

while the probability density function (PDF) is given by

$$f_{d_i}(x) = \frac{2x}{R^2 - r^2}, \quad x \in [r, R]. \qquad (4)$$

Setting $r = 0$ in the aforementioned expressions, the CDF and the PDF of the distance for the case of the sources being uniformly and homogeneously distributed in a circular disk are derived, thus the provided analysis is general enough to capture the circular disk case.

To fully understand the examined network and derive important design insights, it is necessary to examine its performance under varying access dynamics. Specifically, assessing its performance under CF and CB schemes becomes pivotal, as each scheme, with its distinct access mechanism, influences the system performance.

A. CONTENTION-FREE ACCESS

The CF access scheme is particularly suited for scenarios where deterministic access is preferred. In this approach, two sources access the channel simultaneously in a specific time slot, while SIC serves as the detection technique, i.e., decoding and subtracting the strongest signal to allow for the decoding of weaker ones. In this case, the achievable rate of the i-th source depends on which source's message is decoded first. Specifically, if its message is decoded first, taking into consideration the interference from the j-th source's signal, the achievable rate is given by

$$R_{i,1} = B \log_2 \left(1 + \frac{\gamma_i}{\gamma_j + 1} \right), \qquad (5)$$

where B denotes the available bandwidth. If its message is decoded second, then the achievable rate is given by

$$R_{i,2} = B \log_2 \left(1 + \frac{\gamma_i}{\epsilon \gamma_j + 1} \right), \qquad (6)$$

where $\epsilon \in \{0, 1\}$ represents the result of the first decoding.

B. CONTENTION-BASED ACCESS

In the CB access scheme, sources compete for channel access in a stochastic manner, leading to scenarios where either multiple sources or just a single source may access the channel in any given time slot. However, this randomness introduces challenges, especially in managing potential collisions and ensuring efficient communication. To address these challenges, the SA-SIC approach, a combination of SA and SIC, is used, which effectively reduces collisions, and thus, enhances network reliability, by mitigating interference during simultaneous transmissions by two sources.

Delving deeper into the CB access scheme, at the start of each frame, the BS transmits a preamble packet. This packet aids in frame synchronization and informs sources about the available RA slots in that frame. To further clarify the RA mechanism, we consider the random variable $I_i \in \{0, 1\}$ defined as the outcome of a Bernoulli trial, where

$$I_i(t) = \begin{cases} 1, & \text{with probability } q_i \\ 0, & \text{with probability } 1 - q_i. \end{cases} \qquad (7)$$

The access probability of I_i, represented as $\mathbb{E}[I_i] = q_i$, indicates a scenario where the i-th source transmits information in a specific time slot.

In the context of SA, it is noteworthy that the probability of K sources accessing the channel simultaneously is determined by the product of N Bernoulli trials. This probability is given by the probability mass function of the Poisson binomial distribution, i.e.,

$$\Pr(K = k) = \sum_{A \in F_k} \prod_{i \in A} q_i \prod_{j \in A^c} (1 - q_i), \qquad (8)$$

where F_k denotes the set of all subsets of k integers that can be selected from $\{1, 2, \ldots, N\}$. Here, A is an ordered subset of F_k with elements in increasing order, and A^c represents its complement. Given this setup, for the case when only the i-th source accesses the channel in a time slot, the achievable rate for this source is given as

$$R_i = B \log_2(1 + \gamma_i). \qquad (9)$$

However, considering that multiple sources compete for channel access and the inherent features of SA-SIC, the achievable rates for two simultaneous source transmissions are defined by (5) and (6).

C. PROPOSED POLICIES

Building upon the CF and CB schemes, in what follows, we propose appropriate policies for mMTC, eMBB, and hybrid mMTC-eMBB scenarios, focusing on both homogeneous and heterogeneous requirements and enabling geometry-aware resource management.

As it has already been mentioned, CF access is preferred for eMBB applications. Hereinafter, two different policies will be considered:

- *eMBB policy 1:* The two eMBB devices that are scheduled to transmit information using the same resource block are located in the same ring around the BS.

- *eMBB policy 2:* The two eMBB devices that are scheduled to transmit information using the same resource block are located in different rings around the BS.

It is noted that by investigating the performance of the aforementioned policies, we can develop optimal user-pairing methods for CF access, offering valuable insights for improved network planning in 6G wireless systems.

On the other hand, CB access is preferred for mMTC applications. Hereinafter, two different policies are proposed:

- *mMTC policy 1:* All mMTC devices are allocated with the same access probability, regardless of their distance from the BS.
- *mMTC policy 2:* The cell is divided in concentric non-overlapping rings around the BS and a different value of access probability is assigned to mMTC devices that are located in different rings. It is noted that this policy is motivated by the fact that the devices located far away from the BS are expected to have higher outage probability. Thus, retaining the same access probability for all devices could have a negative impact on throughput or fairness among sources.

Finally, a policy for applications with heterogeneous types of services is proposed:

- *Hybrid mMTC-eMBB policy:* An eMBB device located in a fixed position shares its dedicated resource block with a number of randomly deployed mMTC devices.

To investigate the performance of the aforementioned policies, it is sufficient to investigate the outage probability in solely three different cases:

- *Case 1:* The i-th source is randomly and uniformly distributed in a circular ring with the BS as the center, while the j-th source is located at a constant distance from the BS.
- *Case 2:* The two sources are deployed homogeneously in concentric non-overlapping rings around the BS.
- *Case 3:* The sources are randomly and uniformly deployed in the same ring around the BS.
  The assumption that the deployment takes place in a ring, makes the analysis wider, as by setting the inner radius of the ring $r = 0$ m the special of distribution in a circle can be investigated.

IV. PERFORMANCE ANALYSIS

In the following analysis, it is assumed that the optimal decoding order for SIC is used, which results in optimal system performance in terms of outage probability and is given by

$$\mathcal{D} = \begin{cases} (i, j), & \frac{\gamma_i}{\gamma_j+1} \geq \beta_i \text{ and } \frac{\gamma_j}{\gamma_i+1} < \beta_j \\ (j, i), & \frac{\gamma_i}{\gamma_j+1} < \beta_i \text{ and } \frac{\gamma_j}{\gamma_i+1} \geq \beta_j \\ (i, j) \text{ or } (j, i), & \text{otherwise,} \end{cases} \quad (10)$$

where $\mathcal{D} = (i, j)$ denotes the decoding order if the i-th source is decoded first and the j-th source is decoded second. It should be highlighted that the optimal decoding order is affected by both the target rate and the existing

channel conditions of the sources. Considering the CF and CB schemes and the various source deployment scenarios, it becomes crucial to quantify the network reliability and performance under these configurations. Therefore, in this section, the outage and throughput performance of the considered network are investigated for the three aforementioned cases. It should be highlighted that outage probability analysis directly applies to the CF scheme, but is also used in the definition of the throughput for both CF and CB schemes. Hence, to evaluate the outage probability, we consider the threshold for the i-th source as

$$\beta_i = 2^{\frac{\hat{R}_i}{B}} - 1, \quad (11)$$

where $\hat{R}_i$ denotes the target rate of the i-th source.

A. OUTAGE PERFORMANCE FOR CASE 1
In the following theorem, the outage probability of the i-th source for case 1 is provided.

Theorem 1: The outage probability of the i-th source for case 1, when i-th and j-th sources access the channel, is given by

$$P_{ij} = \Phi_1 - \Phi_2 + \Phi_3 + \Phi_4, \quad (12)$$

where

$$\Phi_1 = 1 - e^{-\frac{\sigma^2 \beta_j d_j^n}{c p_j}} \quad (13)$$

and the expressions for Φ_2, Φ_3, and Φ_4 are obtained from Tables 1, 2, and 3, respectively, where $x = \sqrt[n]{\frac{p_i}{\beta_i p_j}}$ and $y = \sqrt[n]{\frac{\beta_j p_i}{p_j}}$.

Proof: The proof is provided in Appendix A. ∎

Remark 1: As observed in Tables 1, 2, and 3, the outage probability depends on the thresholds of the two sources and the distance between the j-th source and the BS. Specifically, the leftmost condition in each table concerns the product of the thresholds for each of the sources, which affects (34), as shown in Appendix A. The other conditions appearing in these tables, on which the expressions depend, include all the possible relations between the distance d_j of the j-th source from the BS and the radii r and R of the ring in which the i-th source is located.

B. OUTAGE PERFORMANCE FOR CASE 2
Next, case 2 is investigated in terms of outage probability. When the sources are positioned uniformly in rings and Rayleigh fading is assumed, the CDF of the channel gain $|h|^2$ is given by [14]

$$F_{|h|^2}(y) = \frac{2}{R^2 - r^2} \int_r^R \left(1 - e^{-\frac{z^n \sigma^2}{c p_i} y}\right) z \, dz, \quad (14)$$

which can be calculated for $n = 2$, but for $n > 2$ being often the case in communication networks, (14) cannot be evaluated. To simplify this expression, the Gauss-Chebyshev

TABLE 1. Cases for Φ_2.

Conditions		Term	Expressions
$\beta_i\beta_j \geq 1$	$d_j x > R$	Φ_2^{11}	$\frac{2}{R^2-r^2}\sum_{k=0}^{\infty}\binom{-1}{k}\left(\frac{p_id_j^n}{p_j\beta_i}\right)^{-k}\frac{\gamma\left(\frac{nk+2}{n},\frac{\sigma^2\beta_iR^n}{cp_i}\right)-\gamma\left(\frac{nk+2}{n},\frac{\sigma^2\beta_ir^n}{cp_i}\right)}{n\left(\frac{\sigma^2\beta_i}{cp_i}\right)^{\frac{nk+2}{n}}}$
	$d_j x < r$	Φ_2^{21}	$\frac{2}{R^2-r^2}\sum_{k=0}^{\infty}\binom{-1}{k}\left(\frac{p_id_j^n}{p_j\beta_i}\right)^{k+1}\frac{\gamma\left(\frac{2-nk-n}{n},\frac{\sigma^2\beta_iR^n}{cp_i}\right)-\gamma\left(\frac{2-nk-n}{n},\frac{\sigma^2\beta_ir^n}{cp_i}\right)}{n\left(\frac{\sigma^2\beta_i}{cp_i}\right)^{\frac{2-nk-n}{n}}}$
	$r < d_j x < R$	Φ_2^{31}	$\frac{2}{R^2-r^2}\sum_{k=0}^{\infty}\binom{-1}{k}\left(\frac{p_id_j^n}{p_j\beta_i}\right)^{-k}\frac{\gamma\left(\frac{nk+2}{n},\frac{\sigma^2\beta_i(d_jx)^n}{cp_i}\right)-\gamma\left(\frac{nk+2}{n},\frac{\sigma^2\beta_ir^n}{cp_i}\right)}{n\left(\frac{\sigma^2\beta_i}{cp_i}\right)^{\frac{nk+2}{n}}}$ $+\frac{2}{R^2-r^2}\sum_{k=0}^{\infty}\binom{-1}{k}\left(\frac{p_id_j^n}{p_j\beta_i}\right)^{k+1}\frac{\gamma\left(\frac{2-nk-n}{n},\frac{\sigma^2\beta_iR^n}{cp_i}\right)-\gamma\left(\frac{2-nk-n}{n},\frac{\sigma^2\beta_i(d_jx)^n}{cp_i}\right)}{n\left(\frac{\sigma^2\beta_i}{cp_i}\right)^{\frac{2-nk-n}{n}}}$
$\beta_i\beta_j < 1$	$d_j x > R$	Φ_2^{12}	$\Phi_2^{11}-\frac{2}{R^2-r^2}\sum_{k=0}^{\infty}\binom{-1}{k}\left(\frac{p_id_j^n}{p_j\beta_i}\right)^{-k}e^{-\frac{\sigma^2\beta_j(\beta_i+1)d_j^n}{(1-\beta_i\beta_j)cp_j}}\frac{\gamma\left(\frac{nk+2}{n},\frac{\sigma^2\beta_i(\beta_j+1)R^n}{(1-\beta_i\beta_j)cp_i}\right)-\gamma\left(\frac{nk+2}{n},\frac{\sigma^2\beta_i(\beta_j+1)r^n}{(1-\beta_i\beta_j)cp_i}\right)}{n\left(\frac{\sigma^2\beta_i(\beta_j+1)}{(1-\beta_i\beta_j)cp_i}\right)^{\frac{nk+2}{n}}}$
	$d_j x < r$	Φ_2^{22}	$\Phi_2^{21}-\frac{2}{R^2-r^2}\sum_{k=0}^{\infty}\binom{-1}{k}\left(\frac{p_id_j^n}{p_j\beta_i}\right)^{k+1}e^{-\frac{\sigma^2\beta_j(\beta_i+1)d_j^n}{(1-\beta_i\beta_j)cp_j}}\frac{\gamma\left(\frac{2-nk-n}{n},\frac{\sigma^2\beta_i(\beta_j+1)R^n}{(1-\beta_i\beta_j)cp_i}\right)-\gamma\left(\frac{2-nk-n}{n},\frac{\sigma^2\beta_i(\beta_j+1)r^n}{(1-\beta_i\beta_j)cp_i}\right)}{n\left(\frac{\sigma^2\beta_i(\beta_j+1)}{(1-\beta_i\beta_j)cp_i}\right)^{\frac{2-nk-n}{n}}}$
	$r < d_j x < R$	Φ_2^{32}	$\Phi_2^{31}-\frac{2}{R^2-r^2}\sum_{k=0}^{\infty}\binom{-1}{k}\left(\frac{p_id_j^n}{p_j\beta_i}\right)^{-k}e^{-\frac{\sigma^2\beta_j(\beta_i+1)d_j^n}{(1-\beta_i\beta_j)cp_j}}\frac{\gamma\left(\frac{nk+2}{n},\frac{\sigma^2\beta_i(\beta_j+1)(d_jx)^n}{(1-\beta_i\beta_j)cp_i}\right)-\gamma\left(\frac{nk+2}{n},\frac{\sigma^2\beta_i(\beta_j+1)r^n}{(1-\beta_i\beta_j)cp_i}\right)}{n\left(\frac{\sigma^2\beta_i(\beta_j+1)}{(1-\beta_i\beta_j)cp_i}\right)^{\frac{nk+2}{n}}}$ $-\frac{2}{R^2-r^2}\sum_{k=0}^{\infty}\binom{-1}{k}\left(\frac{p_id_j^n}{p_j\beta_i}\right)^{k+1}e^{-\frac{\sigma^2\beta_j(\beta_i+1)d_j^n}{(1-\beta_i\beta_j)cp_j}}\frac{\gamma\left(\frac{2-nk-n}{n},\frac{\sigma^2\beta_i(\beta_j+1)R^n}{(1-\beta_i\beta_j)cp_i}\right)-\gamma\left(\frac{2-nk-n}{n},\frac{\sigma^2\beta_i(\beta_j+1)(d_jx)^n}{(1-\beta_i\beta_j)cp_i}\right)}{n\left(\frac{\sigma^2\beta_i(\beta_j+1)}{(1-\beta_i\beta_j)cp_i}\right)^{\frac{2-nk-n}{n}}}$

quadrature approximation is implemented, thus (14) can be written as

$$F_{|h|^2}(y) \approx \frac{1}{R+r}\sum_{n=1}^{M}w_nh(\theta_n),\qquad(15)$$

where

$$h(x)=\sqrt{1-x^2}\left(1-e^{-\frac{\sigma^2}{cp_i}\left(\frac{R-r}{2}x+\frac{R+r}{2}\right)^2y}\right)$$
$$\times\left(\frac{R-r}{2}x+\frac{R+r}{2}\right),\qquad(16)$$

with M being a parameter adjusting the accuracy and complexity of the approximation, $w_n=\frac{\pi}{M}$, and $\theta(n)=\cos(\frac{2n-1}{2M}\pi)$.

The outage probability of the i-th source, when both sources are distributed uniformly in non-overlapping rings and their distance from the BS is considered as a random variable is defined as [20]

$$P_{ij}=\underbrace{\Pr\left(\frac{\gamma_i}{\gamma_j+1}<\beta_i,\frac{\gamma_j}{\gamma_i+1}<\beta_j\right)}_{P_1}$$
$$+\underbrace{\Pr\left(\frac{\gamma_j}{\gamma_i+1}\geq\beta_j,\gamma_j<\beta_i\right)}_{P_2}.\qquad(17)$$

Theorem 2: The outage probability for case 2, when i-th and j-th sources access the channel, is given as

$$P_{ij}=F_{11}^1+F_{11}^1-F_{12}^1-F_{12}^2+F_{21}-F_{22}^1-F_{22}^2,\qquad(18)$$

where the above expressions are presented in Table 4,

$$g(r,R,p,n)=\frac{\sigma^2}{pc}\left(\frac{R-r}{2}\theta(n)+\frac{R+r}{2}\right)^n,\qquad(19)$$

$$f(r,R,n)=\frac{1}{R+r}\frac{\pi}{M}\sqrt{1-\theta(n)^2}\left(\frac{R-r}{2}\theta(n)+\frac{R+r}{2}\right),\qquad(20)$$

and

$$\xi=\begin{cases}\frac{(\beta_i+1)\beta_j}{1-\beta_i\beta_j}, & \beta_i\beta_j<1\\\infty, & \beta_i\beta_j\geq1.\end{cases}\qquad(21)$$

Proof: The proof is provided in Appendix B. ∎

Remark 2: In case 2, the sources are deployed in non overlapping rings, thus there are no conditions concerning their radii. Moreover, considering ξ, it should be highlighted that if $\beta_i\beta_j\geq1$, the expressions are simplified, since the terms including ξ in the exponent are equal to 0.

C. OUTAGE PERFORMANCE FOR CASE 3
In case 3, the outage probability, when both sources are randomly deployed in the same ring, is calculated.

TABLE 2. Cases for Φ_3.

	Conditions	Term	Expressions
$\beta_i\beta_j \geq 1$	$d_j y > R$	Φ_3^{11}	$\dfrac{2}{R^2-r^2}\sum_{k=0}^{\infty}\binom{-1}{k}\left(\dfrac{p_i\beta_j d_j^n}{p_j}\right)^{-k}e^{-\frac{\sigma^2\beta_j d_j^n}{cp_j}}\dfrac{R^{nk+2}-r^{nk+2}}{nk+2}$
	$d_j y < r$	Φ_3^{21}	$\dfrac{2}{R^2-r^2}\sum_{k=0}^{\infty}\binom{-1}{k}\left(\dfrac{p_i\beta_j d_j^n}{p_j}\right)^{k+1}e^{-\frac{\sigma^2\beta_j d_j^n}{cp_j}}\dfrac{R^{2-nk-n}-r^{2-nk-n}}{2-nk-n}$
	$r < d_j y < R$	Φ_3^{31}	$\dfrac{2}{R^2-r^2}\sum_{k=0}^{\infty}\binom{-1}{k}\left(\dfrac{p_i\beta_j d_j^n}{p_j}\right)^{-k}e^{-\frac{\sigma^2\beta_j d_j^n}{cp_j}}\dfrac{(d_j y)^{nk+2}-r^{nk+2}}{nk+2}$ $+\dfrac{2}{R^2-r^2}\sum_{k=0}^{\infty}\binom{-1}{k}\left(\dfrac{p_i\beta_j d_j^n}{p_j}\right)^{k+1}e^{-\frac{\sigma^2\beta_j d_j^n}{cp_j}}\dfrac{R^{2-nk-n}-(d_j y)^{2-nk-n}}{2-nk-n}$
$\beta_i\beta_j < 1$	$d_j y > R$	Φ_3^{12}	$\Phi_3^{11}-\dfrac{2}{R^2-r^2}\sum_{k=0}^{\infty}\binom{-1}{k}\left(\dfrac{p_i\beta_j d_j^n}{p_j}\right)^{-k}e^{-\frac{\sigma^2\beta_j(\beta_i+1)d_j^n}{(1-\beta_i\beta_j)cp_j}}\dfrac{\gamma\left(\frac{nk+2}{n},\frac{\sigma^2\beta_i(\beta_j+1)R^n}{(1-\beta_i\beta_j)cp_i}\right)-\gamma\left(\frac{nk+2}{n},\frac{\sigma^2\beta_i(\beta_j+1)r^n}{(1-\beta_i\beta_j)cp_i}\right)}{n\left(\frac{\sigma^2\beta_i(\beta_j+1)}{(1-\beta_i\beta_j)cp_i}\right)^{\frac{nk+2}{n}}}$
	$d_j y < r$	Φ_3^{22}	$\Phi_3^{21}-\dfrac{2}{R^2-r^2}\sum_{k=0}^{\infty}\binom{-1}{k}\left(\dfrac{p_i\beta_j d_j^n}{p_j}\right)^{k+1}e^{-\frac{\sigma^2\beta_j(\beta_i+1)d_j^n}{(1-\beta_i\beta_j)cp_j}}$ $\times\dfrac{\gamma\left(\frac{2-nk-n}{n},\frac{\sigma^2\beta_i(\beta_j+1)R^n}{(1-\beta_i\beta_j)cp_i}\right)-\gamma\left(\frac{2-nk-n}{n},\frac{\sigma^2\beta_i(\beta_j+1)r^n}{(1-\beta_i\beta_j)cp_i}\right)}{n\left(\frac{\sigma^2\beta_i(\beta_j+1)}{(1-\beta_i\beta_j)cp_i}\right)^{\frac{2-nk-n}{n}}}$
	$r < d_j y < R$	Φ_3^{32}	$\Phi_3^{31}-\dfrac{2}{R^2-r^2}\sum_{k=0}^{\infty}\binom{-1}{k}\left(\dfrac{p_i\beta_j d_j^n}{p_j}\right)^{-k}e^{-\frac{\sigma^2\beta_j(\beta_i+1)d_j^n}{(1-\beta_i\beta_j)cp_j}}\dfrac{\gamma\left(\frac{nk+2}{n},\frac{\sigma^2\beta_i(\beta_j+1)(d_j y)^n}{(1-\beta_i\beta_j)cp_i}\right)-\gamma\left(\frac{nk+2}{n},\frac{\sigma^2\beta_i(\beta_j+1)r^n}{(1-\beta_i\beta_j)cp_i}\right)}{n\left(\frac{\sigma^2\beta_i(\beta_j+1)}{(1-\beta_i\beta_j)cp_i}\right)^{\frac{nk+2}{n}}}$ $-\dfrac{2}{R^2-r^2}\sum_{k=0}^{\infty}\binom{-1}{k}\left(\dfrac{p_i\beta_j d_j^n}{p_j}\right)^{k+1}e^{-\frac{\sigma^2\beta_j(\beta_i+1)d_j^n}{(1-\beta_i\beta_j)cp_j}}\dfrac{\gamma\left(\frac{2-nk-n}{n},\frac{\sigma^2\beta_i(\beta_j+1)R^n}{(1-\beta_i\beta_j)cp_i}\right)-\gamma\left(\frac{2-nk-n}{n},\frac{\sigma^2\beta_i(\beta_j+1)(d_j y)^n}{(1-\beta_i\beta_j)cp_i}\right)}{n\left(\frac{\sigma^2\beta_i(\beta_j+1)}{(1-\beta_i\beta_j)cp_i}\right)^{\frac{2-nk-n}{n}}}$

TABLE 3. Cases for Φ_4.

Condition	Expressions
$d_j y > R$	$\dfrac{2}{R^2-r^2}\sum_{k=0}^{\infty}\binom{-1}{k}\left(\dfrac{p_i\beta_j d_j^n}{p_j}\right)^{-1-k}e^{-\frac{\sigma^2\beta_j d_j^n}{cp_j}}\dfrac{R^{nk+n+2}-r^{nk+n+2}}{nk+n+2}$ $-\dfrac{2}{R^2-r^2}\sum_{k=0}^{\infty}\binom{-1}{k}\left(\dfrac{p_i\beta_j d_j^n}{p_j}\right)^{-1-k}e^{-\frac{\sigma^2\beta_j(\beta_i+1)d_j^n}{cp_j}}\dfrac{\gamma\left(\frac{nk+n+2}{n},\frac{\sigma^2\beta_i R^n}{cp_i}\right)-\gamma\left(\frac{nk+n+2}{n},\frac{\sigma^2\beta_i r^n}{cp_i}\right)}{n\left(\frac{\sigma^2\beta_i}{cp_i}\right)^{\frac{nk+n+2}{n}}}$
$d_j y < r$	$\dfrac{2}{R^2-r^2}\sum_{k=0}^{\infty}\binom{-1}{k}\left(\dfrac{p_i\beta_j d_j^n}{p_j}\right)^{k}e^{-\frac{\sigma^2\beta_j d_j^n}{cp_j}}\dfrac{R^{-nk+2}-r^{-nk+2}}{-nk+2}$ $-\dfrac{2}{R^2-r^2}\sum_{k=0}^{\infty}\binom{-1}{k}\left(\dfrac{p_i\beta_j d_j^n}{p_j}\right)^{k}e^{-\frac{\sigma^2\beta_j(\beta_i+1)d_j^n}{cp_j}}\dfrac{\gamma\left(\frac{-nk+2}{n},\frac{\sigma^2\beta_i R^n}{cp_i}\right)-\gamma\left(\frac{-nk+2}{n},\frac{\sigma^2\beta_i r^n}{cp_i}\right)}{n\left(\frac{\sigma^2\beta_i}{cp_i}\right)^{\frac{-nk+2}{n}}}$
$r < d_j y < R$	$\dfrac{2}{R^2-r^2}\sum_{k=0}^{\infty}\binom{-1}{k}\left(\dfrac{p_i\beta_j d_j^n}{p_j}\right)^{-1-k}e^{-\frac{\sigma^2\beta_j d_j^n}{cp_j}}\dfrac{(d_j y)^{nk+n+2}-r^{nk+n+2}}{nk+n+2}$ $+\dfrac{2}{R^2-r^2}\sum_{k=0}^{\infty}\binom{-1}{k}\left(\dfrac{p_i\beta_j d_j^n}{p_j}\right)^{k}e^{\frac{\sigma^2\beta_j d_j^n}{cp_j}}\dfrac{R^{-nk+2}-(d_j y)^{-nk+2}}{-nk+2}$ $-\dfrac{2}{R^2-r^2}\sum_{k=0}^{\infty}\binom{-1}{k}\left(\dfrac{p_i\beta_j d_j^n}{p_j}\right)^{-1-k}e^{-\frac{\sigma^2\beta_j(\beta_i+1)d_j^n}{cp_j}}\dfrac{\gamma\left(\frac{nk+n+2}{n},\frac{\sigma^2\beta_i(d_j y)^n}{cp_i}\right)-\gamma\left(\frac{nk+n+2}{n},\frac{\sigma^2\beta_i r^n}{cp_i}\right)}{n\left(\frac{\sigma^2\beta_i}{cp_i}\right)^{\frac{nk+n+2}{n}}}$ $-\dfrac{2}{R^2-r^2}\sum_{k=0}^{\infty}\binom{-1}{k}\left(\dfrac{p_i\beta_j d_j^n}{p_j}\right)^{k}e^{-\frac{\sigma^2\beta_j(\beta_i+1)d_j^n}{cp_j}}\dfrac{\gamma\left(\frac{-nk+2}{n},\frac{\sigma^2\beta_i R^n}{cp_i}\right)-\gamma\left(\frac{-nk+2}{n},\frac{\sigma^2\beta_i(d_j y)^n}{cp_i}\right)}{n\left(\frac{\sigma^2\beta_i}{cp_i}\right)^{\frac{-nk+2}{n}}}$

Theorem 3: The outage probability of the i-th source for case 3, when i-th and j-th sources access the channel, is given by

$$P_{ij} = 1 - G_1 - G_2 + G_3 + G_4, \qquad (22)$$

where

$$G_1 = \frac{2}{R^2-r^2}\frac{\gamma\left(\frac{2}{n},\frac{\sigma^2\beta_j R^n}{cp_j}\right)-\gamma\left(\frac{2}{n},\frac{\sigma^2\beta_j r^n}{cp_j}\right)}{n\left(\frac{\sigma^2\beta_j}{cp_j}\right)^{\frac{2}{n}}} \qquad (23)$$

TABLE 4. Expressions for case 2.

Terms		Expression
P_1	F_{11}^1	$\displaystyle\sum_{n=1}^{M}\sum_{m=1}^{M} f(r_1,R_1,n)f(r_2,R_2,m)\left(1 - e^{g(r_2,R_2,p_j,m)\xi}\right)$
	F_{11}^2	$\displaystyle\sum_{n=1}^{M}\sum_{m=1}^{M} f(r_1,R_1,n)f(r_2,R_2,m)\left(\frac{g(r_2,R_2,p_j,m)e^{-g(r_1,R_1,p_i,n)\beta_i}}{g(r_1,R_1,p_i,n)\beta_i + g(r_2,R_2,p_j,m)}\right)\left(1 - e^{-(g(r_1,R_1,p_i,n)\beta_i + g(r_2,R_2,p_j,m))\xi}\right)$
	F_{12}^1	$\displaystyle\sum_{n=1}^{M}\sum_{m=1}^{M} f(r_1,R_1,n)f(r_2,R_2,m)\left(e^{-g(r_2,R_2,p_j,m)\beta_j} - e^{-g(r_2,R_2,p_j,m)\xi}\right)$
	F_{12}^2	$\displaystyle -\sum_{n=1}^{M}\sum_{m=1}^{M} f(r_1,R_1,n)f(r_2,R_2,m)\frac{g(r_2,R_2,p_j,m)e^{g(r_1,R_1,p_i,n)}}{\frac{g(r_1,R_1,p_i,n)}{\beta_j} + g(r_2,R_2,p_j,m)}$ $\displaystyle\times\left(e^{-\left(\frac{g(r_1,R_1,p_i,n)}{\beta_j}+g(r_2,R_2,p_j,m)\right)\xi} - e^{-\left(\frac{g(r_1,R_1,p_i,n)}{\beta_j}+g(r_2,R_2,p_j,m)\right)\beta_j}\right)$
P_2	F_{21}	$\displaystyle\sum_{n=1}^{M} f(r_1,R_1,n)\left(1 - e^{-g(r_1,R_1,p_i,n)\beta_i}\right)$
	F_{22}^1	$\displaystyle\sum_{n=1}^{M}\sum_{m=1}^{M} f(r_1,R_1,n)f(r_2,R_2,m)\left(1 - e^{-g(r_1,R_1,p_i,n)\beta_i}\right)$
	F_{22}^2	$\displaystyle\sum_{n=1}^{M}\sum_{m=1}^{M} f(r_1,R_1,n)f(r_2,R_2,m)\left(\frac{g(r_1,R_1,p_i,n)e^{-g(r_2,R_2,p_j,m)\beta_j}}{g(r_2,R_2,p_j,m)\beta_j + g(r_1,R_1,p_i,n)}\left(1 - e^{-(g(r_2,R_2,p_j,m)\beta_j + g(r_1,R_1,p_i,n))\beta_i}\right)\right)$

and the expressions for G_2, G_3, and G_4 are presented in Table 5, where ζ_1, ζ_2, ζ_3, ζ_4, ζ_5, and ζ_6 are given by (24)–(28) shown at the bottom of the page, and (29) shown at the bottom of the p. 10, with $x = \sqrt[n]{\frac{p_i}{\beta_i p_j}}$ and $y = \sqrt[n]{\frac{\beta_j p_i}{p_j}}$.

Proof: The proof is provided in Appendix C. ∎

Remark 3: Similar to case 1, the first condition in Table 5 concerns the thresholds for each source, which affects the expression for the outage probability. However, in this case, x and y, appearing in the second condition and depending on the transmit powers and the target rates of the sources, affect the limits of the integrals, as shown in Table 7, and consequently the expression for the outage probability.

$$\zeta_1(a_1,a_2,a_3,a_4,a_5,a_6) = \frac{4}{(R^2-r^2)^2}\sum_{k=0}^{\infty}\sum_{m=0}^{\infty}\binom{-1}{k}\left(\frac{\sigma^2}{cp_j}\right)^{a_1}\left(\frac{\sigma^2\beta_i}{cp_i}\right)^{m-a_1}\frac{(-1)^m a_2^{a_3}}{m!a_3}\frac{a_4^{a_5} - a_6^{a_5}}{a_5} \tag{24}$$

$$\zeta_2(a_1,a_2,a_3,a_4,a_5,a_6) = \frac{4}{(R^2-r^2)^2}\sum_{k=0}^{\infty}\sum_{m=0}^{\infty}\binom{-1}{k}\left(\frac{\sigma^2}{cp_j}\right)^{a_1}\left(\frac{\sigma^2\beta_i}{cp_i}\right)^{m-a_1}$$
$$\frac{(-1)^m\left(\frac{\sigma^2\beta_i(\beta_j+1)}{(1-\beta_i\beta_j)cp_i}\right)^m a_2^{a_3}}{m!a_3}\frac{\gamma\left(a_4,\frac{\beta_j(\beta_i+1)\sigma^2 a_5^n}{(1-\beta_i\beta_j)cp_i}\right) - \gamma\left(a_4,\frac{\beta_j(\beta_i+1)\sigma^2 a_6^n}{(1-\beta_i\beta_j)cp_j}\right)}{n\left(\frac{\beta_j(\beta_i+1)\sigma^2}{(1-\beta_i\beta_j)cp_i}\right)^{a_4}} \tag{25}$$

$$\zeta_3(a_1,a_2,a_3,a_4,a_5,a_6) = \frac{4}{(R^2-r^2)^2}\sum_{k=0}^{\infty}\binom{-1}{k}\left(\frac{p_i\beta_j}{p_j}\right)^{a_1}\frac{a_2^{a_3}}{a_3}\frac{\gamma\left(a_4,\frac{\sigma^2\beta_j a_5^n}{cp_j}\right) - \gamma\left(a_4,\frac{\sigma^2\beta_j a_6^n}{cp_j}\right)}{n\left(\frac{\sigma^2\beta_j}{cp_j}\right)^{a_4}} \tag{26}$$

$$\zeta_4(a_1,a_2,a_3,a_4,a_5,a_6) = \frac{4}{(R^2-r^2)^2}\sum_{k=0}^{\infty}\sum_{m=0}^{\infty}\binom{-1}{k}\left(\frac{p_i\beta_j}{p_j}\right)^{a_1}$$
$$\frac{(-1)^m\left(\frac{\sigma^2\beta_i(1+\beta_j)^m}{cp_i(1-\beta_i\beta_j)^m}a_2^{a_3}\right)}{m!a_3}\frac{\gamma\left(a_4,\frac{\sigma^2\beta_j(1+\beta_i)a_5^n}{cp_j(1-\beta_i\beta_j)}\right) - \gamma\left(a_4,\frac{\sigma^2\beta_j(1+\beta_i)a_6^n}{cp_j(1-\beta_i\beta_j)}\right)}{n\left(\frac{\sigma^2\beta_j(1+\beta_i)}{cp_j(1-\beta_i\beta_j)}\right)^{a_4}} \tag{27}$$

$$\zeta_5(a_1,a_2,a_3,a_4,a_5,a_6) = \frac{4}{(R^2-r^2)^2}\sum_{k=0}^{\infty}\binom{-1}{k}\left(\frac{p_i\beta_j}{p_j}\right)^{a_1}\frac{a_2^{a_3}}{a_3}\frac{\gamma\left(a_4,\frac{\sigma^2\beta_j a_5^n}{cp_j}\right) - \gamma\left(a_4,\frac{\sigma^2\beta_j a_6^n}{cp_j}\right)}{n\left(\frac{\sigma^2\beta_j}{cp_j}\right)^{a_4}} \tag{28}$$

TABLE 5. Expressions for case 3.

Terms		Conditions		Expression
G_2	G_2^1	$\beta_i\beta_j \geq 1$	$x < 1$	$\zeta_1\left(-k, x, nk+nm+2, R, nm+4, \frac{r}{x}\right) - \zeta_1\left(-k, r, nk+nm+2, R, -nk+2, \frac{r}{x}\right)$ $+ \zeta_1\left(k+1, R, -nk-n+nm+2, R, nk+n+2, \frac{r}{x}\right) - \zeta_1\left(k+1, x, -nk-n+nm+2, R, nm+4, \frac{r}{x}\right)$ $+ \zeta_1\left(k+1, R, -nk-n+nm+2, \frac{r}{x}, nk+n+2, r\right) - \zeta_1\left(k+1, r, -nk-n+nm+2, \frac{r}{x}, nk+n+2, r\right)$
	G_2^2		$x > 1$	$\zeta_1\left(-k, x, nk+nm+2, \frac{R}{x}, nm+4, r\right) - \zeta_1\left(-k, r, nk+nm+2, \frac{R}{x}, -nk+2, r\right)$ $+ \zeta_1\left(-k, R, nk+nm+2, R, -nk+2, \frac{R}{x}\right) - \zeta_1\left(-k, r, nk+nm+2, R, -nk+2, \frac{R}{x}\right)$ $+ \zeta_1\left(k+1, R, -nk-n+nm+2, \frac{R}{x}, nk+n+2, r\right) - \zeta_1\left(k+1, x, -nk-n+nm+2, \frac{R}{x}, nm+4, r\right)$
	G_2^3	$\beta_i\beta_j < 1$	$x < 1$	$G_2^1 - \zeta_2\left(-k, x, nk+nm+2, \frac{nm+4}{n}, R, \frac{r}{x}\right) + \zeta_2\left(-k, r, nk+nm+2, \frac{-nk+2}{n}, R, \frac{r}{x}\right)$ $- \zeta_2\left(k+1, R, -nk-n+nm+2, \frac{nk+n+2}{n}, R, \frac{r}{x}\right) + \zeta_2\left(k+1, x, -nk-n+nm+2, \frac{nm+4}{n}, R, \frac{r}{x}\right)$ $- \zeta_2\left(k+1, R, -nk-n+nm+2, \frac{nk+n+2}{n}, \frac{r}{x}, r\right) + \zeta_2\left(k+1, r, -nk-n+nm+2, \frac{nk+n+2}{n}, \frac{r}{x}, r\right)$
	G_2^4		$x > 1$	$G_2^2 - \zeta_2\left(-k, x, nk+nm+2, \frac{nm+4}{n}, \frac{R}{x}, r\right) + \zeta_2\left(-k, r, nk+nm+2, \frac{-nk+2}{n}, \frac{R}{x}, r\right)$ $- \zeta_2\left(-k, R, nk+nm+2, \frac{-nk+2}{n}, R, \frac{R}{x}\right) + \zeta_2\left(-k, r, nk+nm+2, \frac{-nk+2}{n}, R, \frac{R}{x}\right)$ $- \zeta_2\left(k+1, R, -nk-n+nm+2, \frac{nk+n+2}{n}, \frac{R}{x}, r\right) + \zeta_2\left(k+1, x, -nk-n+nm+2, \frac{nm+4}{n}, \frac{R}{x}, r\right)$
G_3	G_3^1	$\beta_i\beta_j \geq 1$	$y < 1$	$\zeta_3\left(-k, y, nk+2, \frac{4}{n}, R, \frac{r}{y}\right) - \zeta_3\left(-k, r, nk+2, \frac{-nk+2}{n}, R, \frac{r}{y}\right)$ $+ \zeta_3\left(k+1, R, 2-nk-n, \frac{nk+n+2}{n}, R, \frac{r}{y}\right) - \zeta_3\left(k+1, y, 2-nk-n, \frac{4}{n}, R, \frac{r}{y}\right)$ $+ \zeta_3\left(k+1, R, 2-nk-n, \frac{nk+n+2}{n}, \frac{r}{y}, r\right) - \zeta_3\left(k+1, r, 2-nk-n, \frac{nk+n+2}{n}, \frac{r}{y}, r\right)$
	G_3^2		$y > 1$	$\zeta_3\left(-k, y, nk+2, \frac{4}{n}, \frac{R}{y}, r\right) - \zeta_3\left(-k, r, nk+2, \frac{-nk+2}{n}, \frac{R}{y}, r\right)$ $+ \zeta_3\left(-k, R, nk+2, \frac{-nk+2}{n}, R, \frac{R}{y}\right) - \zeta_3\left(-k, r, nk+2, \frac{-nk+2}{n}, R, \frac{R}{y}\right)$ $+ \zeta_3\left(k+1, R, 2-nk-n, \frac{nk+n+2}{n}, \frac{R}{y}, r\right) - \zeta_3\left(k+1, y, 2-nk-n, \frac{4}{n}, \frac{R}{y}, r\right)$
	G_3^3	$\beta_i\beta_j < 1$	$y < 1$	$G_3^1 - \zeta_4\left(-k, y, nk+nm+2, \frac{nm+4}{n}, R, \frac{r}{y}\right) + \zeta_4\left(-k, r, nk+nm+2, \frac{-nk+2}{n}, R, \frac{r}{y}\right)$ $- \zeta_4\left(k+1, R, -nk-n+nm+2, \frac{nk+n+2}{n}, R, \frac{r}{y}\right) + \zeta_4\left(k+1, y, -nk-n+nm+2, \frac{nm+4}{n}, R, \frac{r}{y}\right)$ $- \zeta_4\left(k+1, R, -nk-n+nm+2, \frac{nk+n+2}{n}, \frac{r}{y}, r\right) + \zeta_4\left(k+1, r, -nk-n+nm+2, \frac{nk+n+2}{n}, \frac{r}{y}, r\right)$
	G_3^4		$y > 1$	$G_3^2 - \zeta_4\left(-k, y, nk+nm+2, \frac{nm+4}{n}, \frac{R}{y}, r\right) + \zeta_4\left(-k, r, nk+nm+2, \frac{-nk+2}{n}, \frac{R}{y}, r\right)$ $- \zeta_4\left(-k, R, nk+nm+2, \frac{-nk+2}{n}, R, \frac{R}{y}\right) + \zeta_4\left(-k, r, nk+nm+2, \frac{-nk+2}{n}, R, \frac{R}{y}\right)$ $- \zeta_4\left(k+1, R, -nk-n+nm+2, \frac{nk+n+2}{n}, \frac{R}{y}, r\right) + \zeta_4\left(k+1, y, -nk-n+nm+2, \frac{nm+4}{n}, \frac{R}{y}, r\right)$
G_4	G_4^1		$y < 1$	$\zeta_5\left(-k-1, y, nk+n+2, \frac{4}{n}, R, \frac{r}{y}\right) - \zeta_5\left(-k-1, r, nk+n+2, \frac{2-nk-n}{n}, R, \frac{r}{y}\right)$ $+ \zeta_5\left(k, R, -nk+2, \frac{nk+2}{n}, R, \frac{r}{y}\right) - \zeta_5\left(k, y, -nk+2, \frac{4}{n}, R, \frac{r}{y}\right)$ $+ \zeta_5\left(k, R, -nk+2, \frac{nk+2}{n}, \frac{r}{y}, r\right) - \zeta_5\left(k, r, -nk+2, \frac{nk+2}{n}, \frac{r}{y}, r\right)$ $- \zeta_6\left(-k-1, y, nk+n+nm+2, \frac{nm+4}{n}, R, \frac{r}{y}\right) + \zeta_6\left(-k-1, r, nk+n+nm+2, \frac{2-nk-n}{n}, R, \frac{r}{y}\right)$ $- \zeta_6\left(k, R, -nk+nm+2, \frac{nk+2}{n}, R, \frac{r}{y}\right) + \zeta_6\left(k, y, -nk+nm+2, \frac{nm+4}{n}, R, \frac{r}{y}\right)$ $- \zeta_6\left(k, R, -nk+nm+2, \frac{nk+2}{n}, \frac{r}{y}, r\right) + \zeta_6\left(k, r, -nk+nm+2, \frac{nk+2}{n}, \frac{r}{y}, r\right)$
	G_4^1		$y > 1$	$\zeta_5\left(-k-1, r, nk+n+2, \frac{4}{n}, \frac{R}{y}, r\right) - \zeta_5\left(-k-1, r, nk+n+2, \frac{2-nk-n}{n}, \frac{R}{y}, r\right)$ $+ \zeta_5\left(-k-1, R, nk+n+2, \frac{2-nk-n}{n}, R, \frac{R}{y}\right) - \zeta_5\left(-k-1, r, nk+n+2, \frac{2-nk-n}{n}, R, \frac{R}{y}\right)$ $+ \zeta_5\left(k, R, -nk+2, \frac{nk+2}{n}, \frac{R}{y}, r\right) - \zeta_5\left(k, y, -nk+2, \frac{4}{n}, \frac{R}{y}, r\right)$ $- \zeta_6\left(-k-1, y, nk+n+nm+2, \frac{nm+4}{n}, \frac{R}{y}, r\right) + \zeta_6\left(-k-1, r, nk+n+nm+2, \frac{2-nk-n}{n}, \frac{R}{y}, r\right)$ $- \zeta_6\left(-k-1, R, nk+n+nm+2, \frac{2-nk-n}{n}, R, \frac{R}{y}\right) + \zeta_6\left(-k-1, r, nk+n+nm+2, \frac{2-nk-n}{n}, R, \frac{R}{y}\right)$ $- \zeta_6\left(k, R, -nk+nm+2, \frac{nk+2}{n}, \frac{R}{y}, r\right) + \zeta_6\left(k, y, -nk+nm+2, \frac{nm+4}{n}, \frac{R}{y}, r\right)$

D. THROUGHPUT ANALYSIS

Next, the throughput of the two considered systems is evaluated, for which the derived expressions for the outage probability are utilized. First, the throughput of the CF system is given by

$$\tilde{R}_i = \hat{R}_i\left(1 - P_{ij}\right), \tag{30}$$

where the target rate $\hat{R}_i$ appears both multiplicatively and in the expression for the outage probability, as indicated by (11).

Regarding the CB system, to evaluate the throughput, the outage probability when only one source accesses the channel is required. The outage probability when the i-th source is distributed in a circular ring and solely accesses the channel is given as

$$P_i = 1 - \frac{2}{R^2 - r^2}\left(\frac{\gamma\left(\frac{2}{n}, \frac{\sigma^2\beta_i R^n}{cp_i}\right) - \gamma\left(\frac{2}{n}, \frac{\sigma^2\beta_i r^n}{cp_i}\right)}{n\left(\frac{\sigma^2\beta_i}{cp_i}\right)^{\frac{2}{n}}}\right). \quad (31)$$

To this end, when the hybrid SA-SIC is utilized, the throughput of the i-th source is given as

$$\tilde{R}_i = \hat{R}_i q_i \prod_{k \neq i}(1 - q_k)(1 - P_i)$$
$$+ \hat{R}_i q_i \sum_{j \neq i} q_j \prod_{k \neq i,j}(1 - q_k)(1 - P_{ij}), \quad (32)$$

It should be noted that the throughput in a system using SA is given as

$$\tilde{R}_i = \hat{R}_i q_i \left(\prod_{k \neq i}(1 - q_k)(1 - P_i)\right). \quad (33)$$

Comparing the two expressions, it can be deduced that the throughput in case of SA-SIC is always greater, due to the second term in (32), which is positive.

E. EXTENSION TO MULTI-ANTENNA SYSTEM

Since an uplink system is investigated, a reasonable extension regarding the number of antennas is the assumption of multiple antennas at the receiver, i.e., a singe-input-multiple-output (SIMO) system. In a SIMO system with maximal-ratio combining (MRC), $\sum_l^L |h_{i,l}|^2$, with L being the number of antennas at the BS, appears in the expressions for the SINR, which follows the gamma distribution considering Rayleigh fading. To this end, since the path loss is not affected by the number of antennas, the analysis of our work can be easily extended to the case of multiple antennas by following the similar procedure and using the gamma distribution instead of the exponential one. This also coincides with assuming Nakagami-m instead of Rayleigh fading. These modifications will uniformly impact system performance without affecting the relative effectiveness or
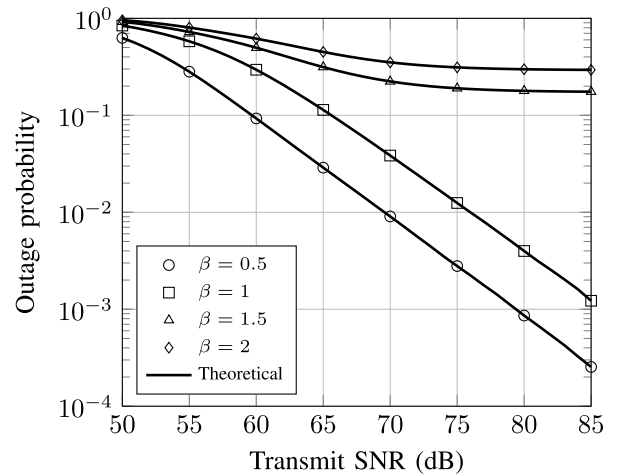

FIGURE 1. Outage probability versus SNR for case 1.

behavioral trends of the considered policies and, thus, the provided insights.

V. NUMERICAL RESULTS AND SIMULATIONS

In this section, we illustrate the performance of the considered network and validate the derived expressions with simulations. We assume the path loss factor is given by (2), with $c = 10^{-3}$ and $n = 2.5$. Furthermore, without loss of generality, it is assumed that the number of sources is $N = 10$ and $q_i = q_j = q_k = \frac{1}{N}$, while $\beta_i = \beta_j = \beta = 2$ unless stated otherwise. Regarding the infinite summations in the expressions for the outage probability in cases 1 and 3, 70 terms are sufficient, while for the expressions in case 2, which includes the Gauss-Chebyshev quadrature approximation 20 terms provide a good approximation. For case 1, it is assumed that $r_i = 5$ m, $R_i = 10$ m, and $d_j = 10$ m, where r_i and R_i denote the inner and outer radii of the ring in which the i-th source is uniformly distributed. For case 2, it is assumed that $r_i = 5$ m, $R_i = 10$ m, $r_j = 10$ m, and $R_j = 20$ m, where r_i, R_i, r_j, and R_j denote the inner and outer radii of the ring in which the i-th and j-th source are located, respectively, while, in case 3, all sources are distributed in a circular ring with $r = 5$ m and $R = 10$ m. It should also be noted that the system throughput refers to the sum throughput of all sources normalized with respect to the number of sources.

In Figs. 1, 2, and 3, the outage probability of the i-th source versus the transmit SNR of the system is presented,

$$\zeta_6(a_1, a_2, a_3, a_4, a_5, a_6) = \frac{4}{(R^2 - r^2)^2}\sum_{k=0}^{\infty}\sum_{m=0}^{\infty}\binom{-1}{k}\left(\frac{p_i\beta_j}{p_j}\right)^{a_1}$$
$$\frac{(-1)^m\left(\frac{\sigma^2\beta_i}{cp_i}\right)a_2^{a_3}}{m!a_3}\frac{\gamma\left(a_4, \frac{\sigma^2\beta_j(\beta_i+1)a_5^n}{cp_j}\right) - \gamma\left(a_4, \frac{\sigma^2\beta_j(\beta_i+1)a_6^n}{cp_j}\right)}{n\left(\frac{\sigma^2\beta_j(\beta_i+1)}{cp_j}\right)^{a_4}} \quad (29)$$
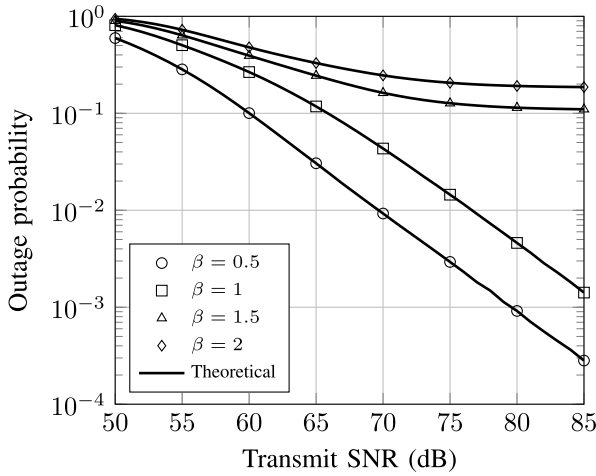
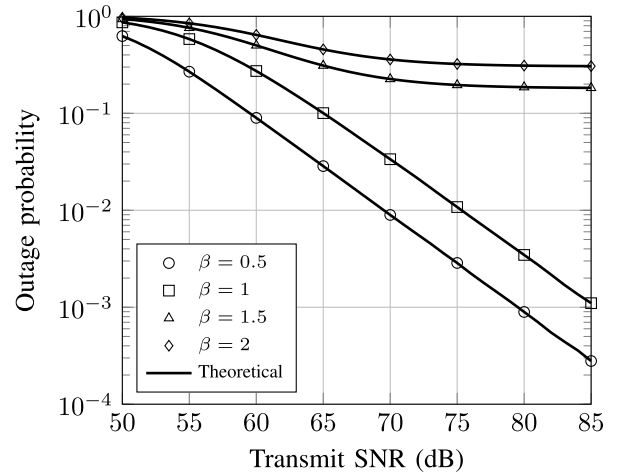**FIGURE 2.** Outage probability versus SNR for case 2.

FIGURE 3. Outage probability versus SNR for case 3.

providing a deeper understanding of the implications of the proposed policies across different cases of the CF system. In Fig. 1, which represents case 1, it becomes evident how the proposed policies can influence system performance as lower threshold values and a higher SNR lead to reduced outage probabilities. Notably, when $\beta_i \beta_j > 1$, a minimum bound on the outage probability is identified, which is absent for $\beta_i \beta_j \leq 1$, emphasizing the efficiency of the policies in managing threshold configurations. Moreover, from Fig. 2, which corresponds to case 2, the position randomness of the j-th source is found to not significantly alter the system performance, indicating a consistent behavior across the scenarios and showcases the adaptability of the proposed policies to varied source deployments. Finally, in Fig. 3, for case 3, where both sources are located in the same ring, the system behavior is similar to that of case 1. Specifically, as the SNR values increase and the β thresholds decrease, outage probabilities are reduced, while notably, a bounded outage probability is evident for $\beta_i \beta_j \geq 1$ at high SNR, further highlighting the robustness of the examined policies. The similarities between the three cases is a result of the comparable values of the corresponding distances and the same thresholds. Finally, it should be highlighted that the average distance of the sources to the base station in case 3 aligns closely with the constant distance in case 1, which results in comparable average system behaviors in both cases. Therefore, the aforementioned figures reveal how the system performance is influenced by the threshold values and source positioning, highlighting the robustness of the investigated system.

In Fig. 4, the hybrid mMTC-eMBB policy is examined and, specifically, the throughput versus q_i for case 1 of the CB system is depicted for various values of SNR. Specifically, we consider a scenario with $N-1$ randomly distributed sources accessing the channel with a probability of q_i, alongside one constantly active fixed-position source, with the system throughput primarily reflecting the performance of the randomly distributed sources. As expected, greater
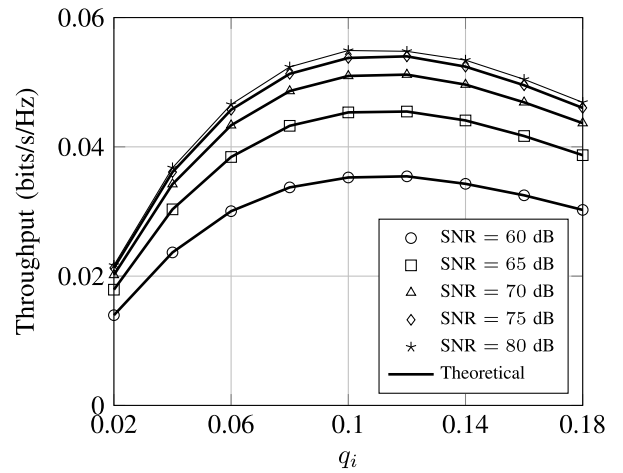
FIGURE 4. System throughput versus q_i for case 1.

values of SNR result in greater throughput for the same value of q_i. In addition, for the presented scenario, the system exhibits a maximum throughput for $q_i = 0.12$, while for greater q_i values the throughput decreases. This decline in performance can be attributed to the increased collision rate and subsequent message loss when the sources access the channel more frequently. Regarding the system throughput and how it is affected by the changes in the SNR, it is observed that as the SNR increases, the maximum throughput tends to stabilize, suggesting that simply increasing the SNR may not always lead to enhanced throughput performance. This conclusion is reached, because, in Fig. 4, while the increment of the SNR is constant the increase of the throughput declines. This can be explained by the throughput expression, where increasing the SNR decreases the outage probability, leading to saturation of the throughput at the fixed target rate.

In Fig. 5, the proposed mMTC policies are directly reflected through a CB system that combines cases 2 and 3. Specifically, we consider a scenario where half of
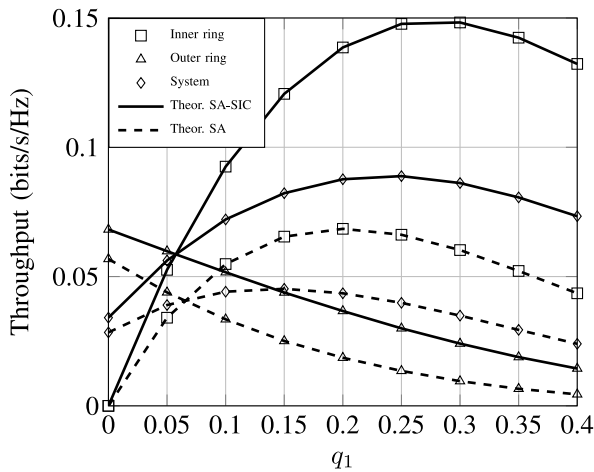
FIGURE 5. System throughput versus q_1 for a practical user-pairing CB scenario.
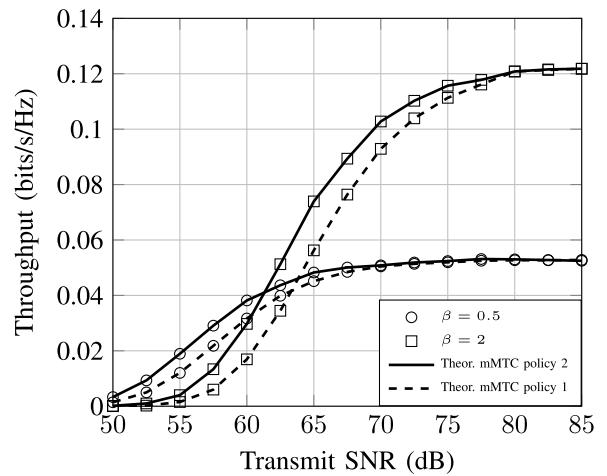

FIGURE 6. Max min system throughput versus SNR for a practical user-pairing CB scenario.

the sources are located in the inner ring accessing with probability q_1, while the sources in the outer ring access with a constant probability q_2, set equal to $\frac{1}{N}$. This setup is in line with mMTC policies which assign the same or different access probabilities based on the device location relative to the BS. Building on this configuration, the figure details the throughput of both an inner and an outer ring source, as well as the overall network throughput, defined as the combined throughput of all sources normalized by their number, plotted against q_1. As it can be seen, across all examined cases, SA-SIC consistently outperforms the SA protocol, proving its superiority and relevance for the proposed policies and scenarios. Furthermore, as q_1 increases, the throughput for the outer ring decreases in both protocols, which is attributed to the reduced availability of free time slots for the outer sources, as the inner ring sources begin to access the channel more frequently. Notably, the throughput for the inner ring, outer ring, and the system peaks at distinct values of q_1, highlighting the significance of tailoring the protocol parameters to the specific policies. In more detail, the throughput for the inner ring peaks at a value of $q_1 = 0.3$, while for the entire system, the optimal throughput is achieved at $q_1 = 0.25$. This slight decrease in the optimal q_1 value for the whole system arises due to the inclusion of the outer ring sources, which have a different access dynamic and influence the overall performance. It should be highlighted that this distinction in optimal values underscores the considerations behind mMTC policies, specifically the need for differentiated access based on proximity to the BS. Finally, the q_1 values that maximize the throughput vary between the SA-SIC and SA cases, highlighting the importance of precise protocol parameter selection.

Fig. 6 illustrates the maximum value of the minimum system throughput versus the transmit SNR for two threshold β values, in a similar user-pairing CB scenario as in Fig. 5. Specifically, the maximum value of the minimum system throughput is derived by considering the access probabilities
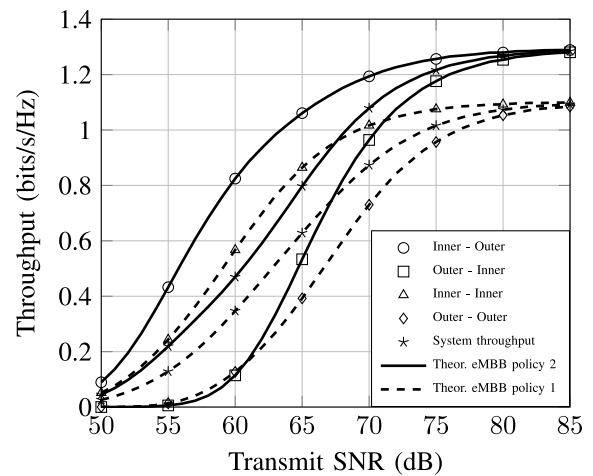

FIGURE 7. System throughput versus SNR for the CF system.

that maximize the system minimum throughput. In more detail, in mMTC policy 1 all sources share a common access probability q, while under mMTC policy 2, the throughput is shaped by two distinct access probabilities q_1 and q_2 for each ring. As it can be seen, mMTC policy 2 consistently offers superior throughput performance, while ensuring fairness among the sources, underscoring the importance of adaptive access strategies. Additionally, Fig. 6 indicates a convergence in the maximum value of the minimum system throughput beyond a specific SNR value, suggesting that merely increasing the transmit SNR might not always enhance performance. It can be observed that reducing the threshold value β leads to a decrease in the SNR at which this convergence initiates, as well as in the peak achievable maximum value of the minimum system throughput. However, for lower SNR values, lower β results in better system performance, which is expected considering that the available power can not consistently support higher target rates.

Finally, in Fig. 7, the performance of a CF system with N sources is investigated. Specifically, half of the sources are

distributed in the inner ring with $r_1 = 5$ m and $R_1 = 10$ m and the other half are located in the outer ring with $r_2 = 10$ m and $R_2 = 20$ m. The comparison is made between the system throughput when sources located in the same ring are paired and its throughput when sources located in different rings are paired. The legend displays the ring in which the i-th and j-th are located, respectively, while the system throughput is calculated by averaging the throughputs of each case. It should be highlighted that the system performs better when the sources are not located in the same ring, i.e., eMBB policy 2 outperforms eMBB policy 1, due to the fact that the impact of the interference can be more easily mitigated by creating pairs with different SNR levels for each source. This result emphasizes the importance of user pairing in such systems. As expected, the higher the SNR the better the system performs, as there is more power allocated for the correct message transmission and, thus, the outage probability is reduced, while the throughput is increased.

VI. CONCLUSION

In this work, we investigated the impact of random source deployment in the context of 6G uplink wireless systems. Specifically, we focused on the implications of non-orthogonality in CF and CB access schemes with both homogeneous and heterogeneous requirements and proposed different policies for mMTC, eMBB, and hybrid mMTC-eMBB scenarios. Regarding the CB scheme, we examined an RA protocol based on SA and SIC termed as SA-SIC. Considering various deployment scenarios ranging from distinct circular rings to a shared ring distribution, we derived closed-form expressions for the outage probability in a system with two sources using SIC. Utilizing these expressions, we also calculated the throughput for each scenario and performed simulations to validate our theoretical findings. Finally, our results confirmed the superior performance of the SA-SIC protocol compared to conventional SA, highlighted the impact of random source deployment in CF and CB access schemes, and provided useful design insights and pairing schemes into the proposed policies for mMTC, eMBB, and hybrid mMTC-eMBB scenarios.

APPENDIX A
PROOF OF THEOREM 1

The outage probability of the i-th source, when two sources access the channel simultaneously and SIC is utilized as the detection technique for constant distances between the sources and the BS, is given by [20]

$$P_{ij} = \underbrace{1 - e^{-b_j \beta_j}}_{\phi_1} - \underbrace{\frac{b_j e^{-b_i \beta_i}}{b_i \beta_i + b_j} c_4}_{\phi_2} + \underbrace{\frac{b_j e^{b_i}}{\frac{b_i}{\beta_j} + b_j} c_5}_{\phi_3}$$
$$+ \underbrace{\frac{b_i e^{-b_j \beta_j}}{b_j \beta_j + b_i} \left(1 - e^{-\beta_i (b_j \beta_j + b_i)} \right)}_{\phi_4}, \tag{34}$$

TABLE 6. Negative binomial series.

Condition	Integral	Expression
$d_j x > R$	$\int_r^R \left(\frac{\sigma^2 d_j^n}{cp_j} + \frac{\sigma^2 \beta_i d_i^n}{cp_i} \right)^{-1} dd_i$	$\sum_{k=0}^{\infty} \binom{-1}{k} \left(\frac{\sigma^2 d_j^n}{cp_j} \right)^{-k-1} \left(\frac{\sigma^2 \beta_i d_i^n}{cp_i} \right)^k$
$d_j x < r$	$\int_r^R \left(\frac{\sigma^2 d_j^n}{cp_j} + \frac{\sigma^2 \beta_i d_i^n}{cp_i} \right)^{-1} dd_i$	$\sum_{k=0}^{\infty} \binom{-1}{k} \left(\frac{\sigma^2 d_j^n}{cp_j} \right)^{k} \left(\frac{\sigma^2 \beta_i d_i^n}{cp_i} \right)^{-k-1}$
$d_j x < R$	$\int_r^{d_j x} \left(\frac{\sigma^2 d_j^n}{cp_j} + \frac{\sigma^2 \beta_i d_i^n}{cp_i} \right)^{-1} dd_i$	$\sum_{k=0}^{\infty} \binom{-1}{k} \left(\frac{\sigma^2 d_j^n}{cp_j} \right)^{-k-1} \left(\frac{\sigma^2 \beta_i d_i^n}{cp_i} \right)^k$
$r < d_j x$	$\int_{d_j x}^R \left(\frac{\sigma^2 d_j^n}{cp_j} + \frac{\sigma^2 \beta_i d_i^n}{cp_i} \right)^{-1} dd_i$	$\sum_{k=0}^{\infty} \binom{-1}{k} \left(\frac{\sigma^2 d_j^n}{cp_j} \right)^{k} \left(\frac{\sigma^2 \beta_i d_i^n}{cp_i} \right)^{-k-1}$

where

$$c_4 = \begin{cases} 1 - e^{-(b_i \beta_i + b_j) \frac{(\beta_i + 1)\beta_j}{1 - \beta_i \beta_j}}, & \beta_i \beta_j < 1 \\ 1, & \beta_i \beta_j \geq 1 \end{cases} \tag{35}$$

and

$$c_5 = \begin{cases} e^{-\beta_j \left(\frac{b_i}{\beta_j} + b_j \right)} - e^{-\left(\frac{b_i}{\beta_j} + b_j \right) \frac{(\beta_i + 1)\beta_j}{1 - \beta_i \beta_j}}, & \beta_i \beta_j < 1 \\ e^{-\beta_j \left(\frac{b_i}{\beta_j} + b_j \right)}, & \beta_i \beta_j \geq 1. \end{cases} \tag{36}$$

To derive the outage probability, (34) should be integrated with respect to $d_i \in [r, R]$. Similar procedure is followed for all terms of (34), thus it is presented indicatively for the second term of (34), for which it stands that

$$\phi_2 = \begin{cases} \frac{\sigma^2 d_j^n}{cp_j} e^{-\frac{\sigma^2 \beta_i d_i^n}{cp_i}} \left(\frac{\sigma^2 \beta_i d_i^n}{cp_i} + \frac{\sigma^2 d_j^n}{cp_j} \right)^{-1}, & \beta_i \beta_j \geq 1 \\ \frac{\sigma^2 d_j^n}{cp_j} e^{-\frac{\sigma^2 \beta_i d_i^n}{cp_i}} \left(\frac{\sigma^2 \beta_i d_i^n}{cp_i} + \frac{\sigma^2 d_j^n}{cp_j} \right)^{-1} \\ \times \left(1 - e^{-\frac{\beta_j(\beta_i + 1)\sigma^2 d_j^n}{(1 - \beta_i \beta_j)cp_j} - \frac{\beta_i \beta_j(\beta_i + 1)\sigma^2 d_i^n}{(1 - \beta_i \beta_j)cp_i}} \right), & \beta_i \beta_j < 1. \end{cases} \tag{37}$$

To integrate this expression, the negative binomial series is required, which arises in the binomial theorem for negative integer exponent and is given by

$$(x + a)^{-n} = \sum_{k=0}^{\infty} \binom{-n}{k} x^k a^{-n-k}, \tag{38}$$

for $|x| < a$. Considering the requirement for convergence during the integration, the cases presented in Table 6 occur. Finally, utilizing [33, (3.381.8)], i.e.,

$$\int_0^u x^m e^{-\beta x^n} dx = \frac{\gamma(\upsilon, \beta u^n)}{n \beta^\upsilon}, \tag{39}$$

where $\upsilon = \frac{m+1}{n}$, the final expressions are derived. Similarly, the rest of the terms are calculated, thus completing the proof.

APPENDIX B
PROOF OF THEOREM 2

Setting in (17) $X = \gamma_i$, $Y = \gamma_j$, the first term turns into

$$P_1 = \Pr\left(\frac{Y}{\beta_j} - 1 < X < \beta_i(Y + 1) \right), \tag{40}$$

TABLE 7. Cases for G_2 (proof).

Conditions			Term	Integral
$\beta_i\beta_j \geq 1$	$r < d_i < d_j x < R$	$x < 1$	G_2^{11}	$\int_{\frac{r}{x}}^{R}\int_{r}^{d_j x}\frac{\sigma^2 d_j^n}{cp_j}e^{-\frac{\sigma^2\beta_i d_i^n}{cp_i}}\left(\frac{\sigma^2\beta_i d_i^n}{cp_i}+\frac{\sigma^2 d_j^n}{cp_j}\right)^{-1}\mathrm{d}d_i\mathrm{d}d_j$
		$x > 1$	G_2^{21}	$\int_{r}^{\frac{R}{x}}\int_{r}^{d_j x}\frac{\sigma^2 d_j^n}{cp_j}e^{-\frac{\sigma^2\beta_i d_i^n}{cp_i}}\left(\frac{\sigma^2\beta_i d_i^n}{cp_i}+\frac{\sigma^2 d_j^n}{cp_j}\right)^{-1}\mathrm{d}d_i\mathrm{d}d_j$
	$r < d_i < R < d_j x$	$x > 1$	G_2^{22}	$\int_{\frac{R}{x}}^{R}\int_{r}^{R}\frac{\sigma^2 d_j^n}{cp_j}e^{-\frac{\sigma^2\beta_i d_i^n}{cp_i}}\left(\frac{\sigma^2\beta_i d_i^n}{cp_i}+\frac{\sigma^2 d_j^n}{cp_j}\right)^{-1}\mathrm{d}d_i\mathrm{d}d_j$
	$r < d_j x < d_i < R$	$x < 1$	G_2^{12}	$\int_{\frac{r}{x}}^{R}\int_{d_j x}^{R}\frac{\sigma^2 d_j^n}{cp_j}e^{-\frac{\sigma^2\beta_i d_i^n}{cp_i}}\left(\frac{\sigma^2\beta_i d_i^n}{cp_i}+\frac{\sigma^2 d_j^n}{cp_j}\right)^{-1}\mathrm{d}d_i\mathrm{d}d_j$
		$x > 1$	G_2^{23}	$\int_{r}^{\frac{R}{x}}\int_{d_j x}^{R}\frac{\sigma^2 d_j^n}{cp_j}e^{-\frac{\sigma^2\beta_i d_i^n}{cp_i}}\left(\frac{\sigma^2\beta_i d_i^n}{cp_i}+\frac{\sigma^2 d_j^n}{cp_j}\right)^{-1}\mathrm{d}d_i\mathrm{d}d_j$
	$d_j x < r < d_i < R$	$x < 1$	G_2^{13}	$\int_{r}^{\frac{r}{x}}\int_{r}^{R}\frac{\sigma^2 d_j^n}{cp_j}e^{-\frac{\sigma^2\beta_i d_i^n}{cp_i}}\left(\frac{\sigma^2\beta_i d_i^n}{cp_i}+\frac{\sigma^2 d_j^n}{cp_j}\right)^{-1}\mathrm{d}d_i\mathrm{d}d_j$
$\beta_i\beta_j < 1$	$r < d_i < d_j x < R$	$x < 1$	G_2^{31}	$\int_{\frac{r}{x}}^{R}\int_{r}^{d_j x}\frac{\sigma^2 d_j^n}{cp_j}e^{-\frac{\sigma^2\beta_i d_i^n}{cp_i}}\left(\frac{\sigma^2\beta_i d_i^n}{cp_i}+\frac{\sigma^2 d_j^n}{cp_j}\right)^{-1}\left(1-e^{-\frac{\beta_j(\beta_i+1)\sigma^2 d_j^n}{cp_j}-\frac{\beta_i(\beta_i\beta_j+\beta_j)\sigma^2 d_i^n}{(1-\beta_i\beta_j)cp_i}}\right)\mathrm{d}d_i\mathrm{d}d_j$
		$x > 1$	G_2^{41}	$\int_{r}^{\frac{R}{x}}\int_{r}^{d_j x}\frac{\sigma^2 d_j^n}{cp_j}e^{-\frac{\sigma^2\beta_i d_i^n}{cp_i}}\left(\frac{\sigma^2\beta_i d_i^n}{cp_i}+\frac{\sigma^2 d_j^n}{cp_j}\right)^{-1}\left(1-e^{-\frac{\beta_j(\beta_i+1)\sigma^2 d_j^n}{cp_j}-\frac{\beta_i(\beta_i\beta_j+\beta_j)\sigma^2 d_i^n}{(1-\beta_i\beta_j)cp_i}}\right)\mathrm{d}d_i\mathrm{d}d_j$
	$r < d_i < R < d_j x$	$x > 1$	G_2^{42}	$\int_{\frac{R}{x}}^{R}\int_{r}^{R}\frac{\sigma^2 d_j^n}{cp_j}e^{-\frac{\sigma^2\beta_i d_i^n}{cp_i}}\left(\frac{\sigma^2\beta_i d_i^n}{cp_i}+\frac{\sigma^2 d_j^n}{cp_j}\right)^{-1}\left(1-e^{-\frac{\beta_j(\beta_i+1)\sigma^2 d_j^n}{cp_j}-\frac{\beta_i(\beta_i\beta_j+\beta_j)\sigma^2 d_i^n}{(1-\beta_i\beta_j)cp_i}}\right)\mathrm{d}d_i\mathrm{d}d_j$
	$r < d_j x < d_i < R$	$x < 1$	G_2^{32}	$\int_{\frac{r}{x}}^{R}\int_{d_j x}^{R}\frac{\sigma^2 d_j^n}{cp_j}e^{-\frac{\sigma^2\beta_i d_i^n}{cp_i}}\left(\frac{\sigma^2\beta_i d_i^n}{cp_i}+\frac{\sigma^2 d_j^n}{cp_j}\right)^{-1}\left(1-e^{-\frac{\beta_j(\beta_i+1)\sigma^2 d_j^n}{cp_j}-\frac{\beta_i(\beta_i\beta_j+\beta_j)\sigma^2 d_i^n}{(1-\beta_i\beta_j)cp_i}}\right)\mathrm{d}d_i\mathrm{d}d_j$
		$x > 1$	G_2^{43}	$\int_{r}^{\frac{R}{x}}\int_{d_j x}^{R}\frac{\sigma^2 d_j^n}{cp_j}e^{-\frac{\sigma^2\beta_i d_i^n}{cp_i}}\left(\frac{\sigma^2\beta_i d_i^n}{cp_i}+\frac{\sigma^2 d_j^n}{cp_j}\right)^{-1}\left(1-e^{-\frac{\beta_j(\beta_i+1)\sigma^2 d_j^n}{cp_j}-\frac{\beta_i(\beta_i\beta_j+\beta_j)\sigma^2 d_i^n}{(1-\beta_i\beta_j)cp_i}}\right)\mathrm{d}d_i\mathrm{d}d_j$
	$d_j x < r < d_i < R$	$x < 1$	G_2^{33}	$\int_{r}^{\frac{r}{x}}\int_{r}^{R}\frac{\sigma^2 d_j^n}{cp_j}e^{-\frac{\sigma^2\beta_i d_i^n}{cp_i}}\left(\frac{\sigma^2\beta_i d_i^n}{cp_i}+\frac{\sigma^2 d_j^n}{cp_j}\right)^{-1}\left(1-e^{-\frac{\beta_j(\beta_i+1)\sigma^2 d_j^n}{cp_j}-\frac{\beta_i(\beta_i\beta_j+\beta_j)\sigma^2 d_i^n}{(1-\beta_i\beta_j)cp_i}}\right)\mathrm{d}d_i\mathrm{d}d_j$

which is equivalent to

$$P_1 = \underbrace{\int_0^\xi F_X(\beta_i(y+1))f_Y(y)\mathrm{d}y}_{F_{11}} - \underbrace{\int_{\beta_j}^\xi F_X\left(\frac{y}{\beta_j}-1\right)f_Y(y)\mathrm{d}y}_{F_{12}}. \tag{41}$$

In (41), the two terms can be written as

$$
\begin{aligned}
F_{11} &= \sum_{n=1}^{M}\sum_{m=1}^{M}f(r_1,R_1,n)f(r_2,R_2,m)\\
&\times \int_0^\xi\left(g(r_2,R_2,p_j,m)e^{-g(r_2,R_2,p_j,m)y}-g(r_2,R_2,p_j,m)\right.\\
&\left.\times e^{-g(r_1,R_1,p_i,n)}e^{-(g(r_1,R_1,p_i,n)bi+g(r_2,R_2,p_j,m))y}\right)\mathrm{d}y
\end{aligned} \tag{42}
$$

and

$$
\begin{aligned}
F_{12} &= \sum_{n=1}^{M}\sum_{m=1}^{M}f(r_1,R_1,n)f(r_2,R_2,m)\\
&\times \int_{\beta_j}^\xi\left(g(r_2,R_2,p_j,m)e^{-g(r_2,R_2,p_j,m)}-g(r_2,R_2,p_j,m)\right.\\
&\left.\times e^{g(r_1,R_1,p_i,n)}e^{-\left(\frac{g(r_1,R_1,p_i,n)}{\beta_j}+g(r_2,R_2,p_j,m)\right)y}\right)\mathrm{d}y.
\end{aligned} \tag{43}
$$

The second term of (17) can be expressed as

$$P_2 = \Pr\left(\frac{Y}{X+1}\geq\beta_j, X\leq\beta_i\right), \tag{44}$$

which is equivalent to

$$P_2 = \underbrace{\int_0^{\beta_i}f_X(x)\mathrm{d}x}_{F_{21}} - \underbrace{\int_0^{\beta_i}F_Y(\beta_j(x+1))f_X(x)\mathrm{d}x}_{F_{22}}. \tag{45}$$

In (45), the two terms can be written as

$$F_{21} = \sum_{n=1}^{M}f(r_1,R_1,n)\int_0^{\beta_i}g(r_1,R_1,p_i,n)e^{-g(r_1,R_1,p_i,n)x}\mathrm{d}x \tag{46}$$

and

$$
\begin{aligned}
F_{22} &= \sum_{n=1}^{M}\sum_{m=1}^{M}f(r_1,R_1,n)f(r_2,R_2,m)\\
&\times \int_0^{\beta_i}\left(g(r_1,R_1,p_i,n)e^{-g(r_1,R_1,p_i,n)x}-g(r_1,R_1,p_i,n)\right.\\
&\left.\times e^{-g(r_2,R_2,p_j,m)\beta_j}e^{-(g(r_2,R_2,p_j,m)\beta_j+g(r_1,R_1,p_i,n))x}\right)\mathrm{d}x.
\end{aligned} \tag{47}
$$

Calculating the integrals, the outage probability is derived and the proof is complete.

APPENDIX C
PROOF OF THEOREM 3

The outage probability of the i-th source, when two sources access the channel simultaneously and they are both randomly deployed in the same ring, is given by

$$P_{ij} = 1 - \underbrace{e^{-b_j \beta_j}}_{g_1} - \underbrace{\frac{b_j e^{-b_i \beta_i}}{b_i \beta_i + b_j} c_4}_{g_2} + \underbrace{\frac{b_j e^{b_i}}{\frac{b_i}{\beta_j} + b_j} c_5}_{g_3}$$

$$+ \underbrace{\frac{b_i e^{-b_j \beta_j}}{b_j \beta_j + b_i} \left(1 - e^{-\beta_i(b_j \beta_j + b_i)}\right)}_{g_4}. \tag{48}$$

To derive the outage probability, (48) is integrated with respect to $d_i \in [r, R]$ and $d_j \in [r, R]$. For g_1, which includes only d_j, a single integration is required, thus

$$G_1 = \frac{2}{R^2 - r^2} \int_r^R d_j e^{-\frac{\sigma^2 \beta_j d_j^n}{cp_j}} \, \mathrm{d}d_j. \tag{49}$$

For the rest of the terms, the procedure is as the one presented indicatively for the second term, for which it stands that

$$g_2 = \begin{cases} \frac{\sigma^2 d_j^n}{cp_j} e^{-\frac{\sigma^2 \beta_i d_i^n}{cp_i}} \left(\frac{\sigma^2 \beta_i d_i^n}{cp_i} + \frac{\sigma^2 d_j^n}{cp_j}\right)^{-1}, & \beta_i \beta_j \geq 1 \\[3mm] \frac{\sigma^2 d_j^n}{cp_j} e^{-\frac{\sigma^2 \beta_i d_i^n}{cp_i}} \left(\frac{\sigma^2 \beta_i d_i^n}{cp_i} + \frac{\sigma^2 d_j^n}{cp_j}\right)^{-1} \\[3mm] \times \left(1 - e^{-\frac{\beta_j(\beta_i+1)\sigma^2 d_j^n}{(1-\beta_i \beta_j)cp_j} - \frac{\beta_i \beta_j(\beta_i+1)\sigma^2 d_i^n}{(1-\beta_i \beta_j)cp_i}}\right), & \beta_i \beta_j < 1. \end{cases} \tag{50}$$

To ensure that the variables range from r to R as well as the convergence of the term $\left(\frac{\sigma^2 d_j^n}{cp_j} + \frac{\sigma^2 \beta_i d_i^n}{cp_i}\right)^{-1}$, the cases presented in Table 7 emerge. To derive the final expressions, we utilize the negative binomial series, [33, (3.381.8)], and [34, (6.5.33)], which completes the proof.

REFERENCES

[1] W. Saad, M. Bennis, and M. Chen, "A vision of 6G wireless systems: Applications, trends, technologies, and open research problems," *IEEE Netw.*, vol. 34, no. 3, pp. 134–142, May/Jun. 2019.

[2] Z. Zhang et al., "6G wireless networks: Vision, requirements, architecture, and key technologies," *IEEE Veh. Technol. Mag.*, vol. 14, no. 3, pp. 28–41, Sep. 2019.

[3] K. David and H. Berndt, "6G vision and requirements: Is there any need for beyond 5G?," *IEEE Veh. Technol. Mag.*, vol. 13, no. 3, pp. 72–80, Sep. 2018.

[4] M. Hasan, E. Hossain, and D. Niyato, "Random access for machine-to-machine communication in LTE-advanced networks: Issues and approaches," *IEEE Commun. Mag.*, vol. 51, no. 6, pp. 86–93, Jun. 2013.

[5] C. Bockelmann et al., "Massive machine-type communications in 5G: Physical and MAC-layer solutions," *IEEE Commun. Mag.*, vol. 54, no. 9, pp. 59–65, Sep. 2016.

[6] J. Kim, J. Lee, J. Kim, and J. Yun, "M2M service platforms: Survey, issues, and enabling technologies," *IEEE Commun. Surveys Tuts.*, vol. 16, no. 1, pp. 61–76, 1st Quart., 2014.

[7] H. Shariatmadari et al., "Machine-type communications: Current status and future perspectives toward 5G systems," *IEEE Commun. Mag.*, vol. 53, no. 9, pp. 10–17, Sep. 2015.

[8] V. Popovsky and B. Tur, "Performance analysis of aloha algorithm," in *Proc. 1st Int. Sci.-Pract. Conf. Probl. Infocommun. Sci. Technol.*, 2014, pp. 21–22.

[9] C. Psomas and I. Krikidis, "Backscatter communications for wireless powered sensor networks with collision resolution," *IEEE Wireless Commun. Lett.*, vol. 6, no. 5, pp. 650–653, Oct. 2017.

[10] D. Tyrovolas et al., "Slotted ALOHA with code combining for IoT networks," in *Proc. IEEE Int. Mediterr. Conf. Commun. Netw. (MeditCom)*, 2023, pp. 164–168.

[11] S. V. Patil, S. Kore, and T. K. Harhare, "A case study: Spectrum efficient multiple access techniques for 5G networks," in *Proc. Int. Conf. Adv. Technol. (ICONAT)*, 2023, pp. 1–4.

[12] V. Ozduran, "Advanced successive interference cancellation for non-orthogonal multiple access," in *Proc. Telecommun. Forum (TELFOR)*, 2018, pp. 1–4.

[13] P. Xu, Z. Ding, X. Dai, and H. V. Poor, "A new evaluation criterion for non-orthogonal multiple access in 5G software defined networks," *IEEE Access*, vol. 3, pp. 1633–1639, 2015.

[14] Z. Ding, Z. Yang, P. Fan, and H. V. Poor, "On the performance of non-orthogonal multiple access in 5G systems with randomly deployed users," *IEEE Signal Process. Lett.*, vol. 21, no. 12, pp. 1501–1505, Dec. 2014.

[15] Z. Chen, Z. Ding, X. Dai, and G. K. Karagiannidis, "On the application of quasi-degradation to MISO-NOMA Downlink," *IEEE Trans. Signal Process.*, vol. 64, no. 23, pp. 6174–6189, Dec. 2016.

[16] Z. Yang, Z. Ding, P. Fan, and G. K. Karagiannidis, "On the performance of non-orthogonal multiple access systems with partial channel information," *IEEE Trans. Commun.*, vol. 64, no. 2, pp. 654–667, Feb. 2016.

[17] Z. Ding, P. Fan, and H. V. Poor, "Impact of user pairing on 5G non-orthogonal multiple-access Downlink transmissions," *IEEE Trans. Veh. Technol.*, vol. 65, no. 8, pp. 6010–6023, Aug. 2016.

[18] J. M. Meredith, "Study on downlink multiuser superposition transmission for LTE," 3GPP, Sophia Antipolis, France, 3GPP Rep. 36.859, 2015.

[19] Z. Wei, L. Yang, D. W. K. Ng, J. Yuan, and L. Hanzo, "On the performance gain of NOMA over OMA in uplink communication systems," *IEEE Trans. Commun.*, vol. 68, no. 1, pp. 536–568, Jan. 2020.

[20] S. A. Tegos, P. D. Diamantoulakis, A. S. Lioumpas, P. G. Sarigiannidis, and G. K. Karagiannidis, "Slotted ALOHA with NOMA for the next generation IoT," *IEEE Trans. Commun.*, vol. 68, no. 10, pp. 6289–6301, Oct. 2020.

[21] P. D. Diamantoulakis, N. D. Chatzidiamantis, A. L. Moustakas, and G. K. Karagiannidis, "Next generation multiple access: Performance gains from uplink MIMO-NOMA," *IEEE Open J. Commun. Soc.*, vol. 3, pp. 2298–2313, 2022.

[22] J. Choi, "NOMA-based random access with multichannel aloha," *IEEE J. Sel. Areas Commun.*, vol. 35, no. 12, pp. 2736–2743, Dec. 2017.

[23] J. Choi, "Layered non-orthogonal random access with SIC and transmit diversity for reliable transmissions," *IEEE Trans. Commun.*, vol. 66, no. 3, pp. 1262–1272, Mar. 2018.

[24] A. Mazin, M. Elkourdi, and R. D. Gitlin, "Comparison of slotted aloha-NOMA and CSMA/CA for M2M communications in IoT networks," in *Proc. IEEE Veh. Technol. Conf. (VTC-Fall)*, 2018, pp. 1–5.

[25] E. Balevi and R. D. Gitlin, "A random access scheme for large scale 5G/IoT applications," in *Proc. IEEE 5G World Forum (5GWF)*, 2018, pp. 452–456.

[26] M. Elkourdi, A. Mazin, E. Balevi, and R. D. Gitlin, "Enabling slotted aloha-NOMA for massive M2M communication in IoT networks," in *Proc. IEEE Wireless Microw. Technol. Conf. (WAMICON)*, 2018, pp. 1–4.

[27] S. N. Chiu, D. Stoyan, W. S. Kendall, and J. Mecke, *Stochastic Geometry and its Applications.* Hoboken, NJ, USA: Wiley, 2013.

[28] F. Baccelli, B. Blaszczyszyn, and P. Muhlethaler, "Stochastic analysis of spatial and opportunistic aloha," *IEEE J. Sel. Areas Commun.*, vol. 27, no. 7, pp. 1105–1119, Sep. 2009.

[29] N. Ehsan and R. L. Cruz, "On the optimal SINR in random access networks with spatial reuse," in *Proc. Annu. Conf. Inf. Sci. Syst.*, 2006, pp. 938–944.

[30] A. Bansal and A. Joshi, "Non orthogonal multiple access in cooperative relay sharing with randomly deployed users," in *Proc. Int. Conf. Commun. Electron. Syst. (ICCES)*, 2019, pp. 1412–1415.

[31] Z. Shi, G. Yang, Y. Fu, H. Wang, and S. Ma, "Performance analysis of MIMO-NOMA systems with randomly deployed users," in *Proc. IEEE Global Commun. Conf. (GLOBECOM)*, 2018, pp. 1–7.

[32] V. K. Papanikolaou, G. K. Karagiannidis, N. A. Mitsiou, and P. D. Diamantoulakis, "Closed-form analysis for NOMA with randomly deployed users in generalized fading," *IEEE Wireless Commun. Lett.*, vol. 9, no. 8, pp. 1253–1257, Aug. 2020.

[33] I. S. Gradshteyn and I. M. Ryzhik, *Table of Integrals, Series, and Products*. Cambridge, MA, USA: Academic, 2014.

[34] M. Abramowitz and I. A. Stegun, *Handbook of Mathematical Functions with Formulas, Graphs, and Mathematical Tables*. vol. 55, Washington, DC, USA: US Govt. Print. off., 1966.

APOSTOLOS A. TEGOS received the Diploma degree (five years) in electrical and computer engineering from the Department of Electrical and Computer Engineering, Aristotle University of Thessaloniki, Thessaloniki, Greece, in 2022, where he is currently pursuing the Ph.D. degree. His current research interests include multiple access in wireless communications, optical wireless communications, and optimization theory.
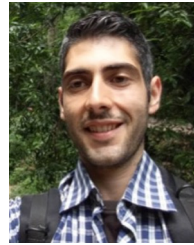
SOTIRIS A. TEGOS (Member, IEEE) received the Diploma (five years) and Ph.D. degrees from the Department of Electrical and Computer Engineering, Aristotle University of Thessaloniki, Thessaloniki, Greece, in 2017 and 2022, respectively.

Since 2022, he has been a Postdoctoral Fellow with the Wireless Communications and Information Processing Group, Aristotle University of Thessaloniki and also with the Department of Applied Informatics, University of Macedonia, Thessaloniki. Since 2023, he has been also a Postdoctoral Fellow with the Department of Electrical and Computer Engineering, University of Western Macedonia, Kozani, Greece. In 2018, he was a Visiting Researcher with the Department of Electrical and Computer Engineering, Khalifa University, Abu Dhabi, UAE. He is a Working Group Member of the Newfocus COST Action "European Network on Future Generation Optical Wireless Communication Technologies." His current research interests include multiple access in wireless communications, wireless power transfer, optical wireless communications, and reconfigurable intelligent surfaces. He received the Best Paper Award in 2023 Photonics Global Conference. He was an Exemplary Reviewer of IEEE WIRELESS COMMUNICATIONS LETTERS in 2019 and 2022 (top 3% of reviewers). He serves as an Associate Editor for IEEE COMMUNICATIONS LETTERS.

DIMITRIOS TYROVOLAS (Graduate Student Member, IEEE) received the Diploma degree (five years) in electrical and computer engineering from the University of Patras, Greece, in 2020. He is currently pursuing the Ph.D. degree with the Department of Electrical and Computer Engineering, Aristotle University of Thessaloniki, Greece. He is also a Research Assistant with the Technical University of Crete, Greece. His current research interests include reconfigurable intelligent surfaces, UAV communications, Internet of Things networks, and probability theory. He was an Exemplary Reviewer of IEEE WIRELESS COMMUNICATIONS LETTERS in 2021 and IEEE COMMUNICATIONS LETTERS in 2022 (top 3% of reviewers).

PANAGIOTIS D. DIAMANTOULAKIS (Senior Member, IEEE) received the Diploma (five years) and Ph.D. degrees from the Department of Electrical and Computer Engineering, Aristotle University of Thessaloniki, Thessaloniki, Greece, in 2012 and 2017, respectively. Since 2022, he has been a Postdoctoral Fellow with the Department of Applied Informatics, University of Macedonia, Thessaloniki. Since 2017, he has been a Postdoctoral Fellow with Wireless Communications and Information Processing Group, AUTH and since 2021, he has been a Visiting Assistant Professor with the Key Laboratory of Information Coding and Transmission, Southwest Jiaotong University, Chengdu, China. His research interests include optimization theory and applications in wireless networks, optical wireless communications, and goal-oriented communications. He is a Working Group Member of the Newfocus COST Action "European Network on Future Generation Optical Wireless Communication Technologies." He serves as an Editor for IEEE OPEN JOURNAL OF THE COMMUNICATIONS SOCIETY, *Physical Communications* (Elsevier), and *Frontiers in Communications and Networks*. From 2018 to 2023, he was an Editor of IEEE WIRELESS COMMUNICATIONS LETTERS. He was also an Exemplary Editor of the IEEE WIRELESS COMMUNICATIONS LETTERS in 2020, and an Exemplary Reviewer of the IEEE COMMUNICATIONS LETTERS in 2014 and the IEEE TRANSACTIONS ON COMMUNICATIONS in 2017 and 2019 (top 3% of reviewers).

PANAGIOTIS SARIGIANNIDIS (Member, IEEE) received the B.Sc. and Ph.D. degrees in computer science from the Aristotle University of Thessaloniki, Thessaloniki, Greece, in 2001 and 2007, respectively. He is the Director of the ITHACA Lab, a Co-Founder of the 1st spin-off of the University of Western Macedonia, Kozani, Greece: MetaMind Innovations P.C., and an Associate Professor with the Department of Electrical and Computer Engineering with the University of Western Macedonia. He has published over 330 papers in international journals, conferences and book chapters. He has been involved in several national, European and international projects, coordinating four H2020/Horizon Europe projects, namely DS-07-2017, SPEAR: Secure And Private Smart Grid; LC-SC3-EC-4-2020, EVIDENT: Behavioral Insgihts and Effective Energy Policy Actions; ICT-56-2020, TERMINET: Next Generation Smart Interconnected IoT; and HORIZON-JU-SNS-2022-STREAM-A-01-06, NANCY: An Artificial Intelligent Aided Unified Network for Secure Beyond 5G Long Term Evolution, while he also coordinates the Operational Program MARS: Smart Farming with Drones (Competitiveness, Entrepreneurship, and Innovation) and the Erasmus+ KA2 ARRANGE-ICT: SmartROOT: Smart Farming Innovation Training. His research interests include telecommunication networks, Internet of Things, and network security. He received six best paper awards and the IEEE SMC TCHS Research and Innovation Award 2023. He serves as a Technical Manager of the H2020-DS-04-2020, ELECTRON: Resilient and Self-Healed Electrical Power Nanogrid, while he served as a Principal Investigator in the H2020-DS04-2018, SDN-microSENSE: SDN-microgrid Resilient Electrical Energy System and in three Erasmus+ KA2: a) ARRANGE-ICT: Partnership for Addressing Megatrends in ICT, b) JAUNTY: Joint Undergaduate Courses for smart Energy Management Systems, and c) STRONG: advanced First Responders Training (Cooperation for Innovation and the Exchange of Good Practices).

GEORGE K. KARAGIANNIDIS (Fellow, IEEE) is currently a Professor with the Electrical and Computer Engineering Department, Aristotle University of Thessaloniki, Greece, and the Head of Wireless Communications and Information Processing Group. He is also a Faculty Fellow with the Artificial Intelligence and Cyber Systems Research Center, Lebanese American University. His research interests are in the areas of wireless communications systems and networks, signal processing, optical wireless communications, wireless power transfer and applications, and communications, and signal processing for biomedical engineering. Recently, he received Three Prestigious Awards: The 2021 IEEE ComSoc RCC Technical Recognition Award, the 2018 IEEE ComSoc SPCE Technical Recognition Award, and the 2022 Humboldt Research Award from Alexander von Humboldt Foundation. He is one of the highly cited authors across all areas of Electrical Engineering, recognized from Clarivate Analytics as a Web of Science Highly Cited Researcher in the nine consecutive years from 2015 to 2023. He was in the past Editor in several IEEE journals and from 2012 to 2015 and he was the Editor-in-Chief of IEEE COMMUNICATIONS LETTERS. From September 2018 to June 2022, he served as an Associate Editor-in-Chief for IEEE OPEN JOURNAL OF COMMUNICATIONS SOCIETY. He is currently in the Steering Committee of IEEE TRANSACTIONS ON COGNITIVE COMMUNICATIONS AND NETWORKS.